

The Climate of (north-central) Chile: Mean state, Variability and Trends

René D. Garreaud

*Department of Geophysics
Universidad de Chile*

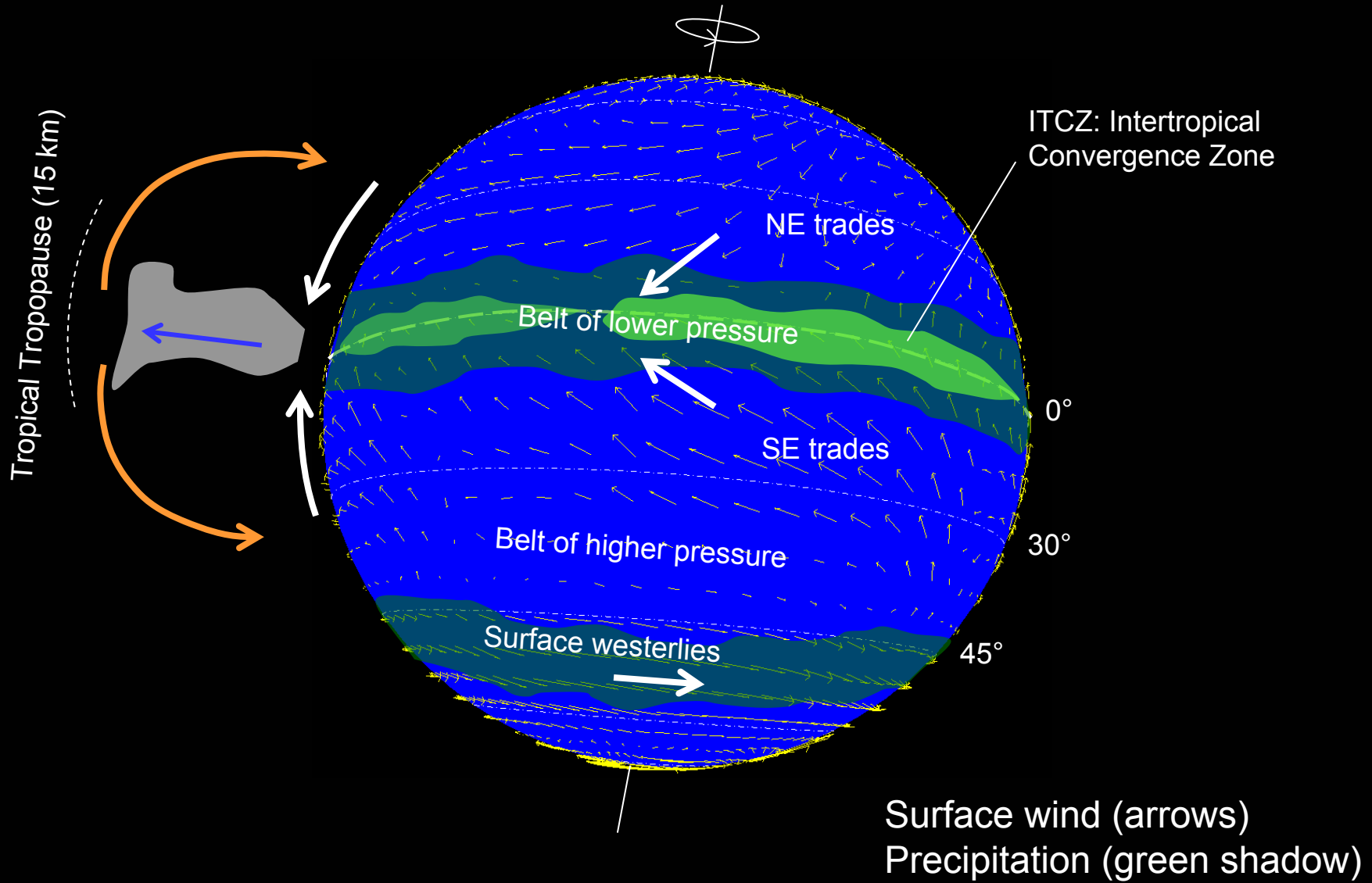
www.dgf.uchile.cl/rene

Astronomical site testing data conference
Valparaiso, Chile, Dec. 1-3, 2010

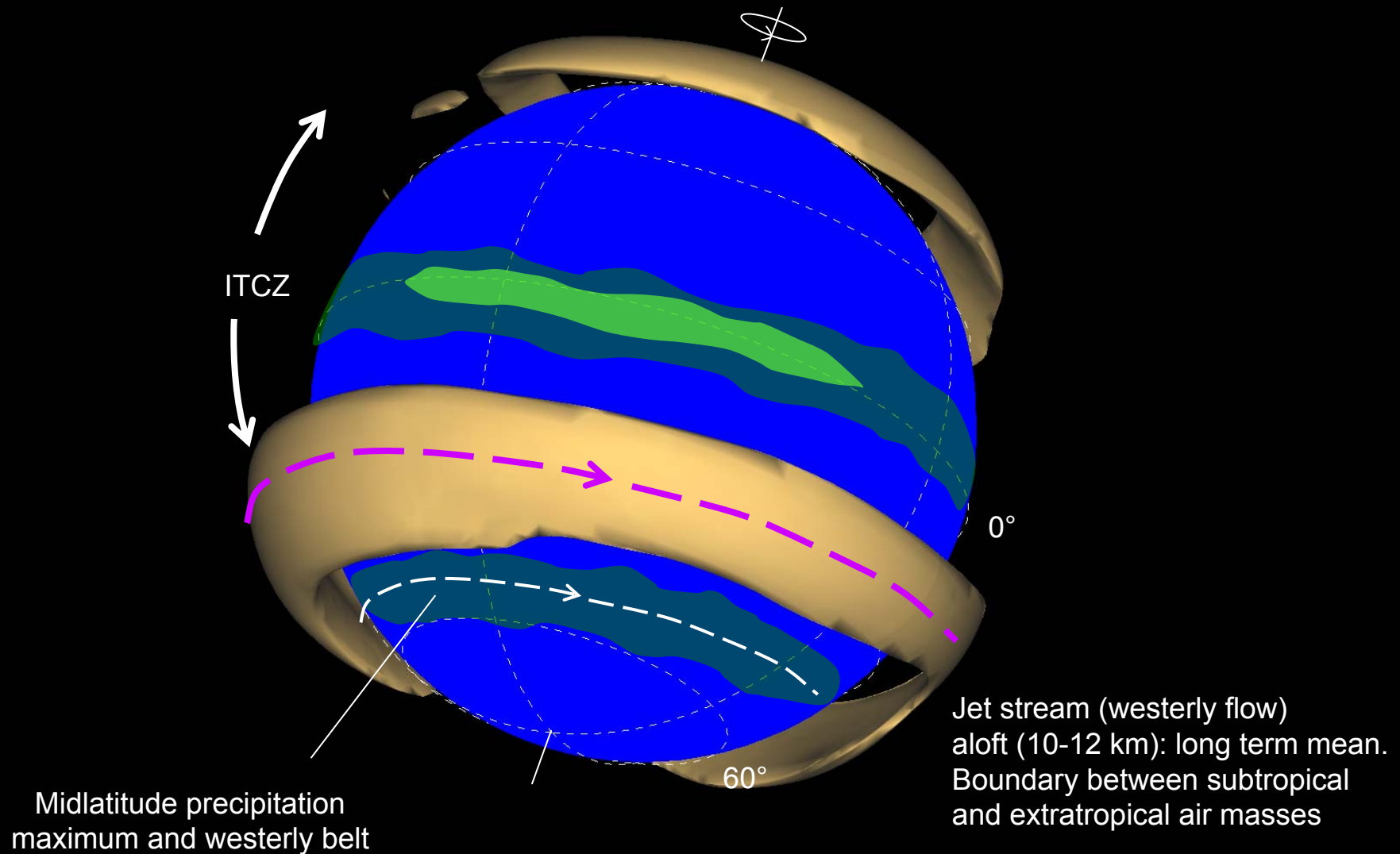
Outline

- Climate background
- Interannual (year-to-year) variability
- Observed trends (last decades)
- Climate projection during the 21st century

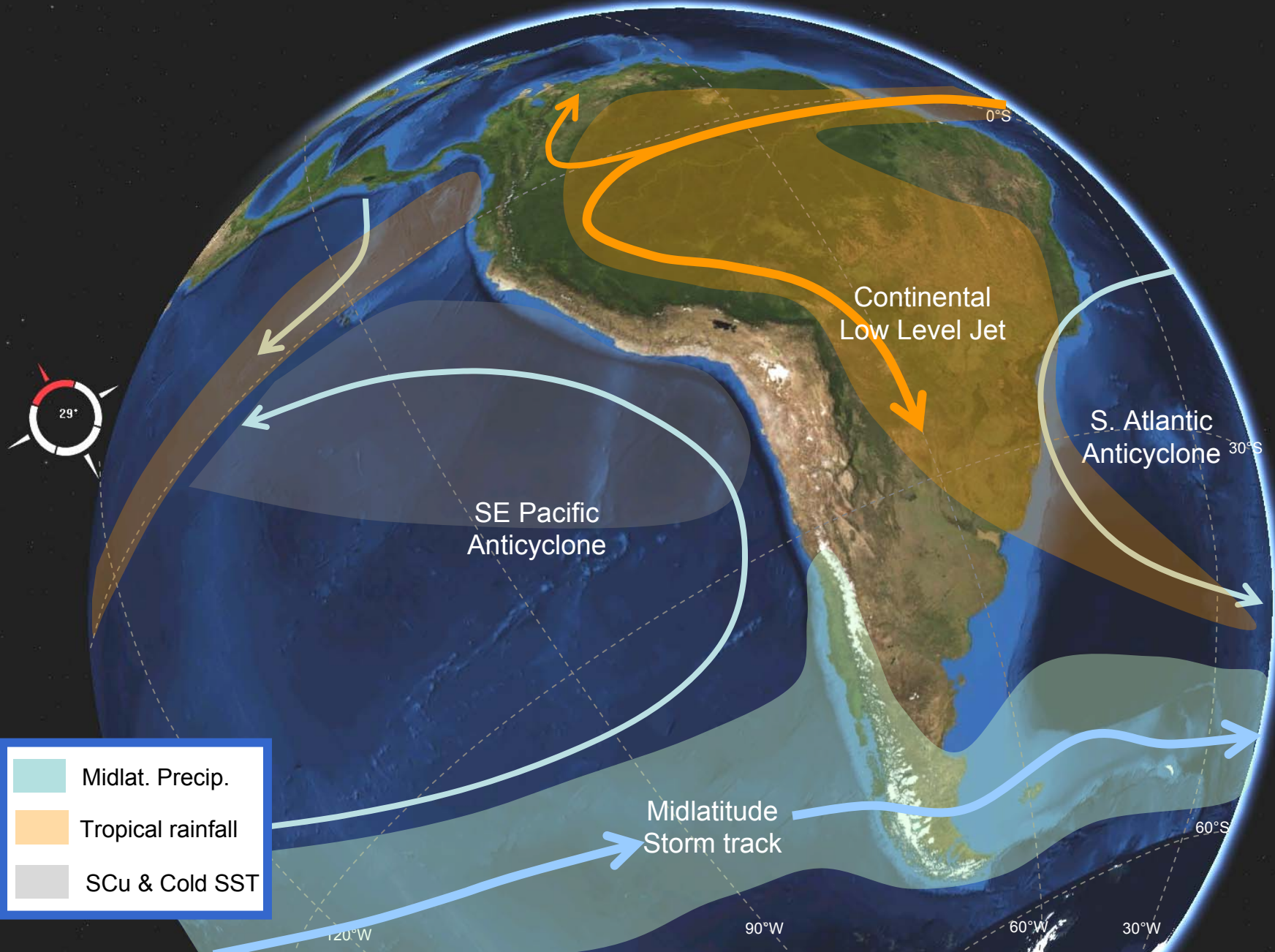
General circulation in an aqua-planet Perpetual Equinox



General circulation in an aqua-planet Perpetual Equinox



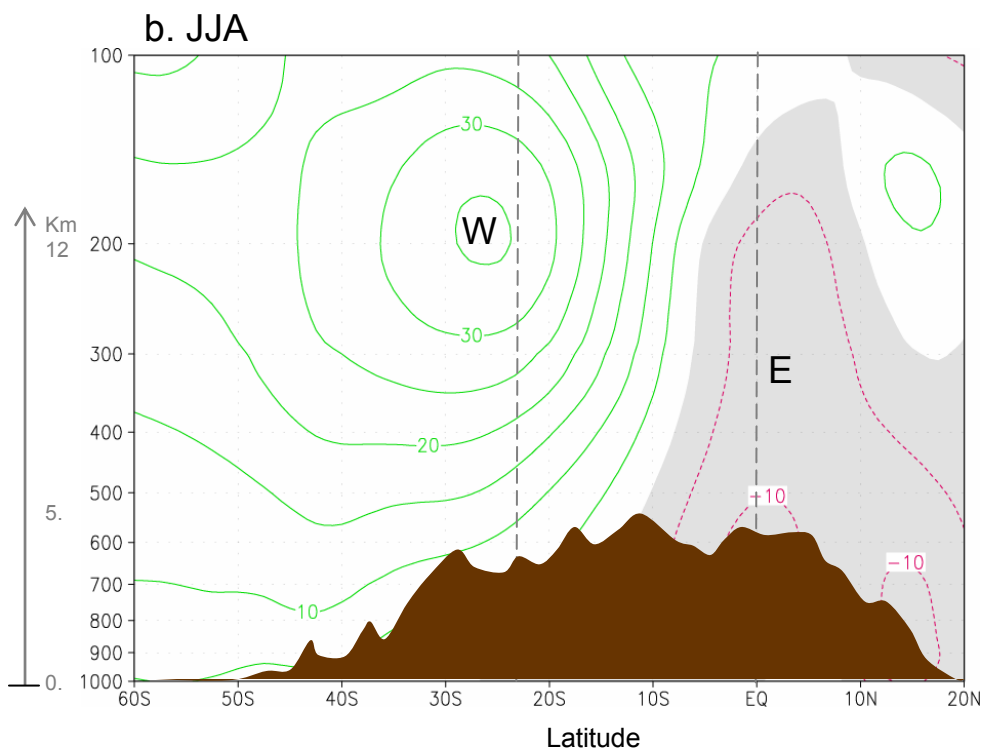
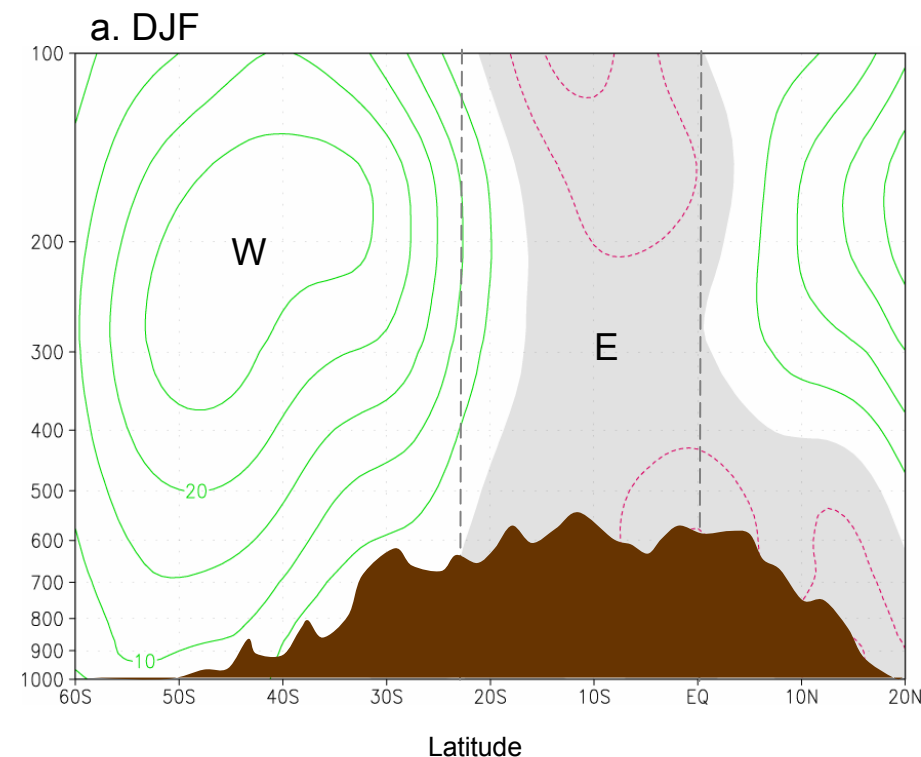
Idealized (zonally symmetric) circulation disturbed by continents



Zonal (east-west) mean flow over the Andes

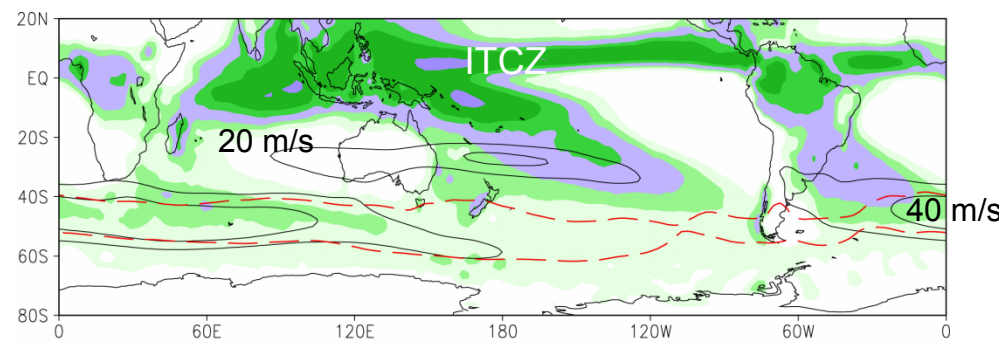
Brown area: Terrain mean height

Dashed line: 500 hPa, half of the atmosphere below!

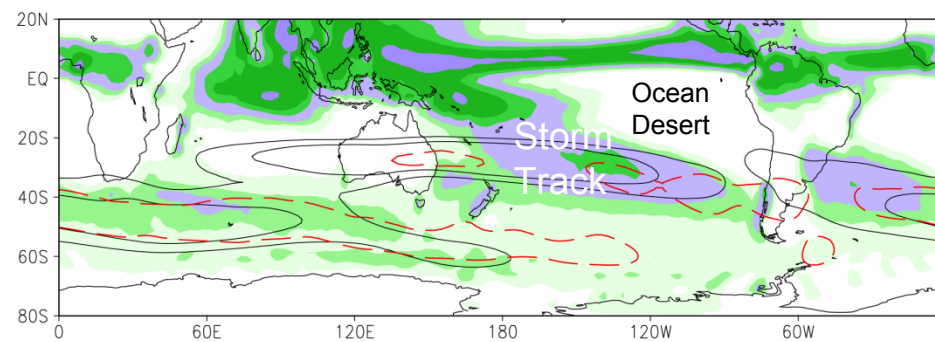


Precipitation and upper level winds

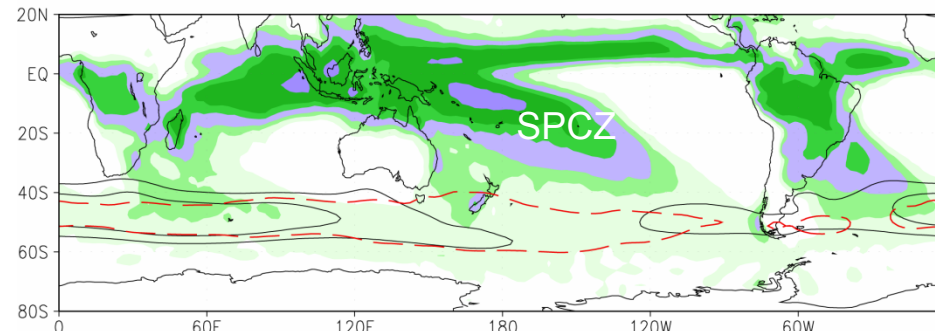
Anual



June

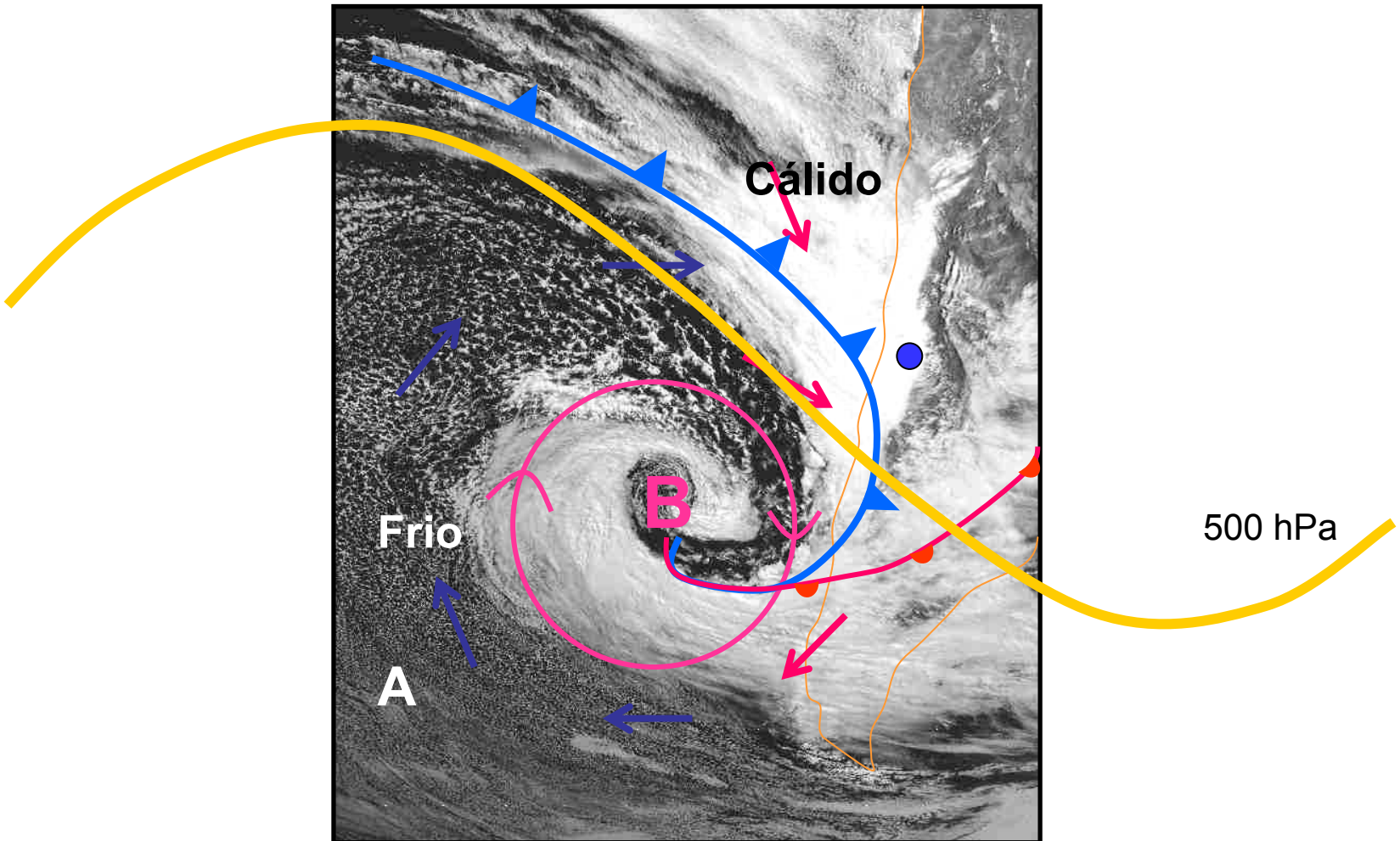


January

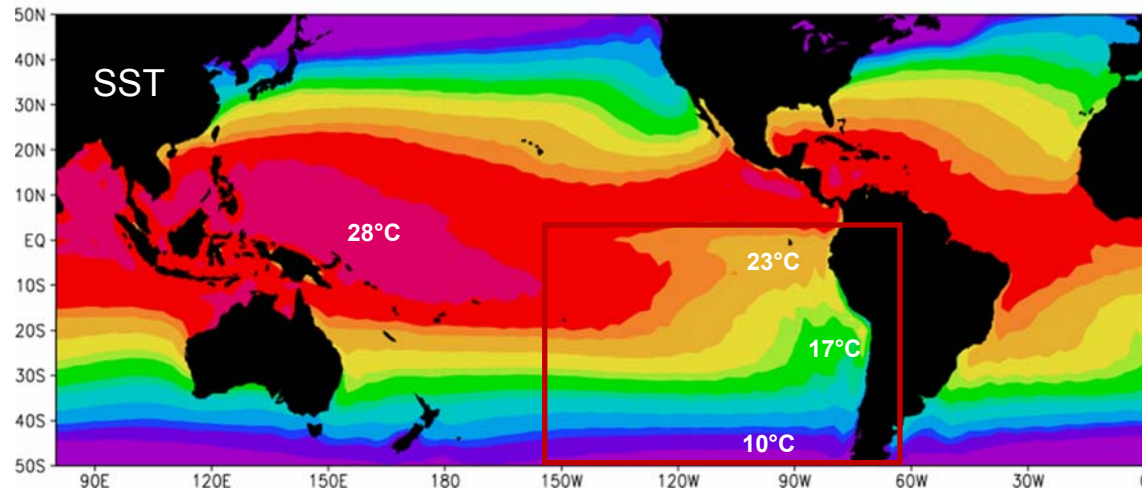
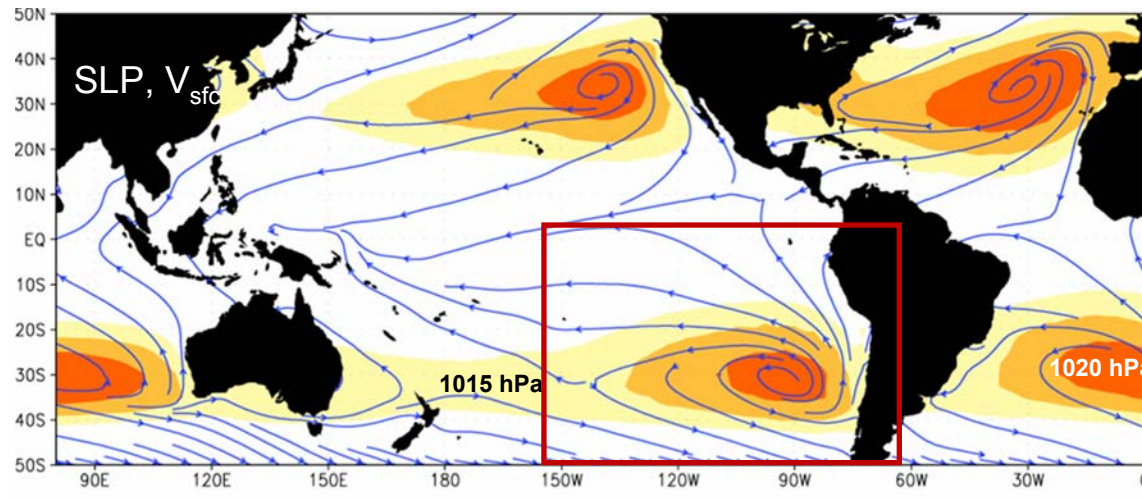


Precipitación en latitudes medias

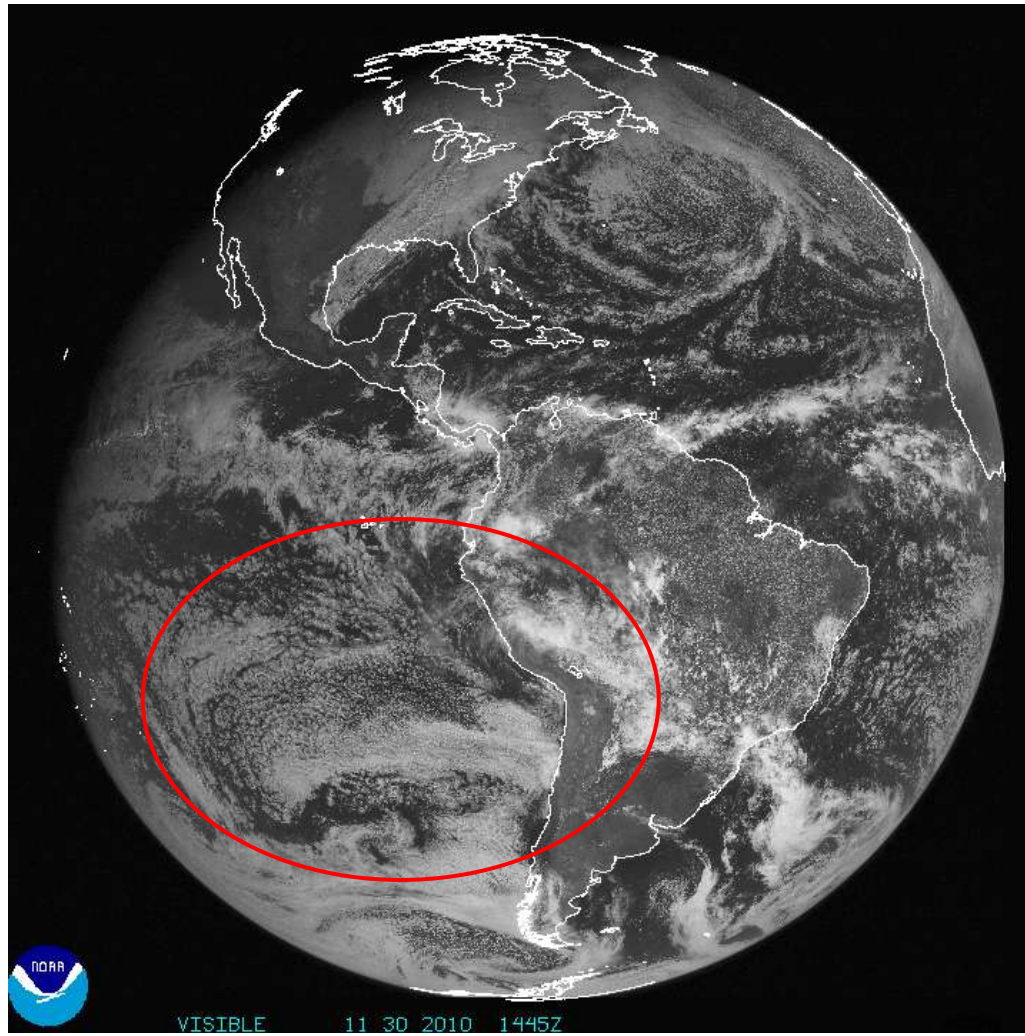
Las perturbaciones de latitudes medias (ver clase anterior) también transportan calor hacia latitudes altas, continuando el proceso de transferencia de calor que realiza la atmósfera.



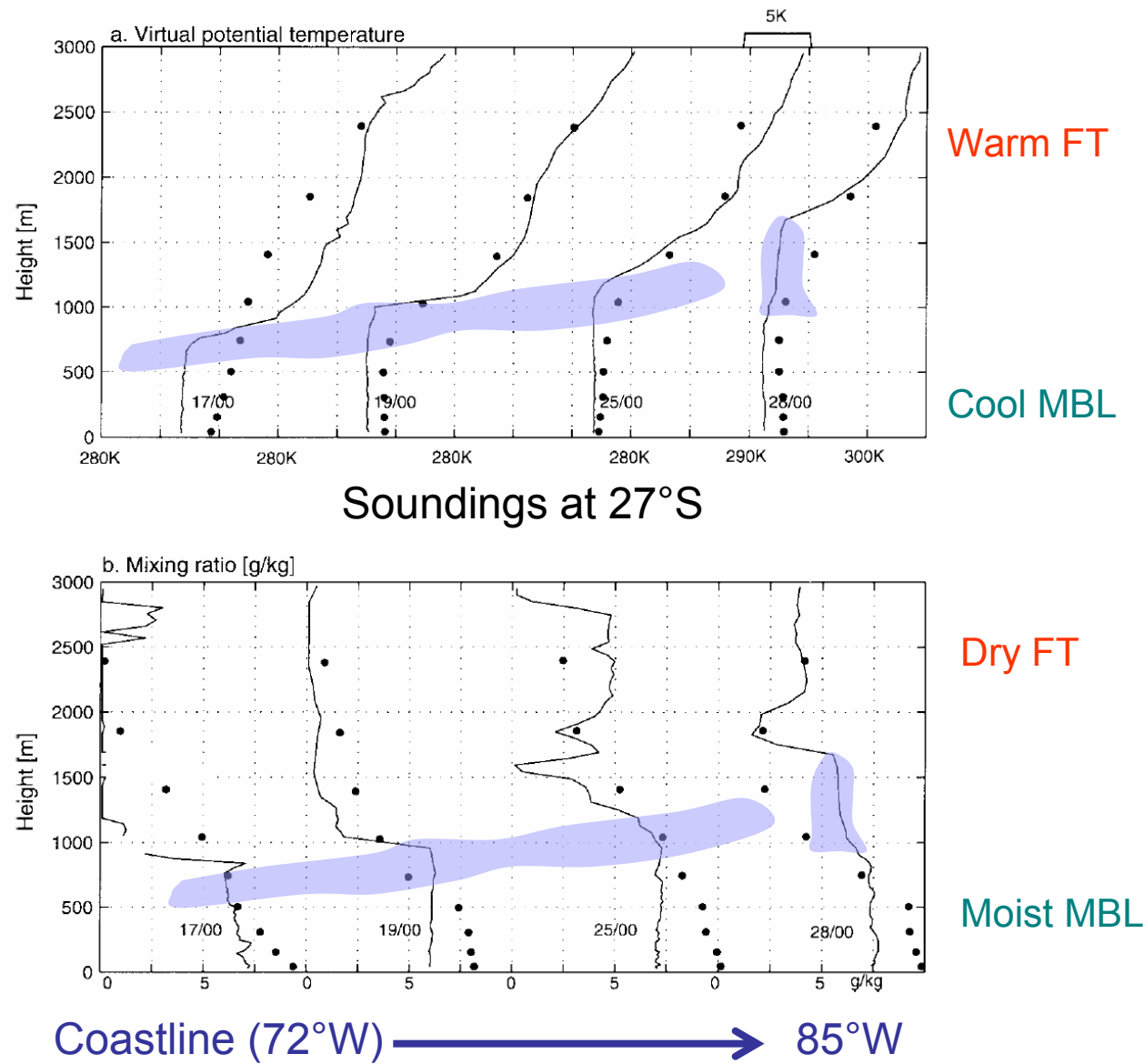
EBUS: Subtropical anticyclones, equatorward flow and cold SST



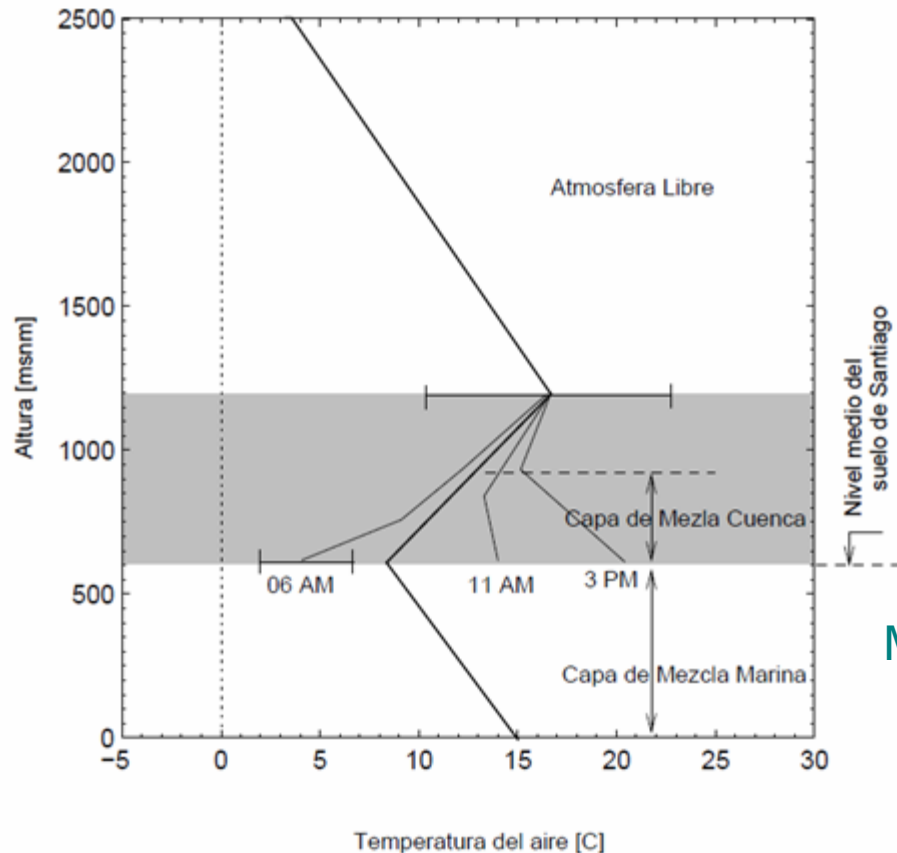
Persistent Stratocumulus cloud deck over the SEP



Persistent Stratocumulus cloud deck over the SEP



Subsidence over SEP distorted by land heating/cooling

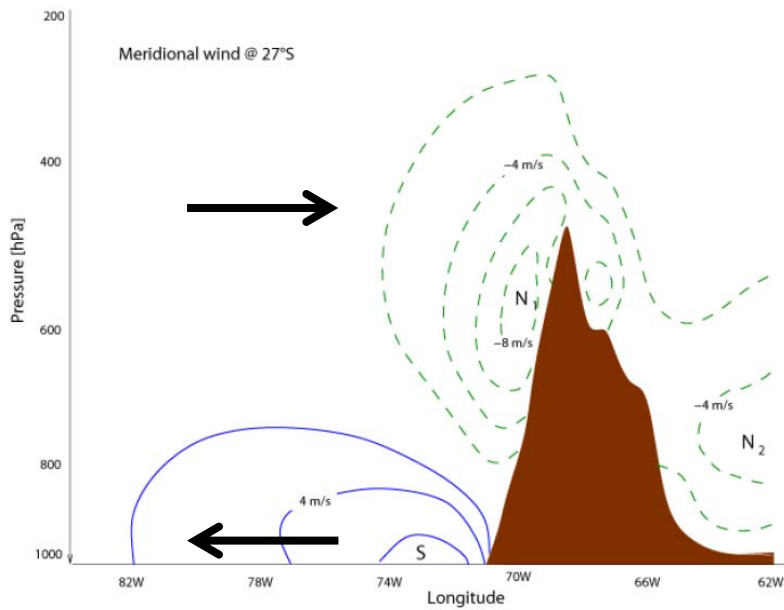


MBL is 1 km deep
at 20°S !

Figure 2: Esquema del perfil vertical de temperatura que típicamente se observa en la zona central de Chile (en torno a los 33°S) sobre la base de los valores medios obtenidos por Rutllant (1994). La línea gruesa representa el perfil sobre la costa. Las líneas delgadas representan el perfil sobre la cuenca de Santiago (nivel del suelo a 600 msnm) a distintas horas del día. El perfil sobre la cuenca coincide con el observado en la costa sobre el tope de la inversión térmica de subsidencia. También se indica el rango de variación típica ($\pm 1\sigma$) de la temperatura mínima en Santiago y la temperatura del tope de la inversión.

Andes mountains disrupt mid-level westerly flow

(a) Meridional wind at 27°S



(b) Wind vectors over Santiago

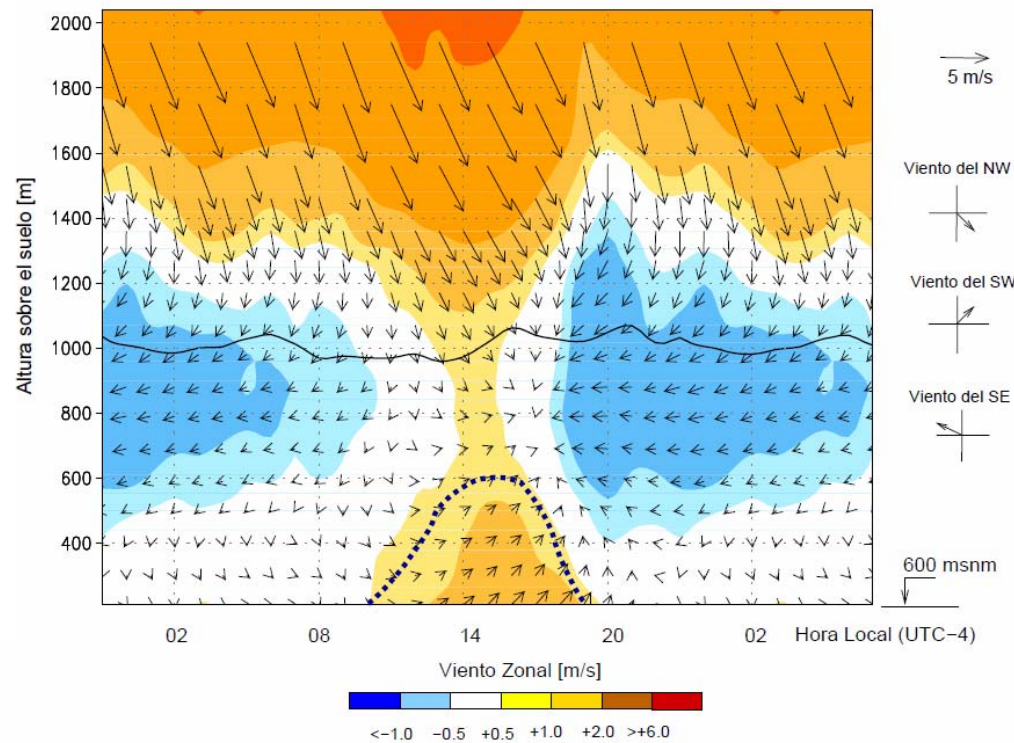


Fig. 4. Pressure-longitude cross section of the meridional wind at 27° S during austral spring (SON). Contour interval is 2 m/s, the zero line is omitted and negative values in dashed lines. The brown area represents the Andes profile at this latitude. To the west of the Andes there is a southerly low-level jet (signalled by an S) just off the coast and a northerly jet (signalled by N1) close to the Andean slope. To the east of the Andes there is evidence of the northerly low-level jet (signalled by N2). Data source: PRECIS simulation of the present day climate.

Garreaud 2009

Figure 4: Diagrama altura-tiempo de los promedios de invierno del viento horizontal (flechas), componente zonal del viento (sombreado) y altura de la capa de mezcla sobre Santiago (línea segmentada gruesa). Los promedios del viento fueron construidos en base a los registros horarios medidos por el perfilador radio-acústico de la Platina (33.5° S, 70.6° W, 620 msnm, suroriente de la ciudad de Santiago) de los meses Mayo a Septiembre del año 1998 y 1999. La magnitud del viento es proporcional al largo de la flecha y su dirección está dada por la orientación de la flecha en forma usual, como se ejemplifica al margen. El sombreado indica la magnitud de la componente zonal según la escala bajo el diagrama. La línea sólida indica la altura en la cual la componente meridional del viento cambia de sur a norte. La altura de la capa de mezcla corresponde al promedio para los meses de invierno obtenida por Ulriksen (1980) sobre la base de mediciones con globos radiosonda.

Andean slope also produces cross-mountain circulations

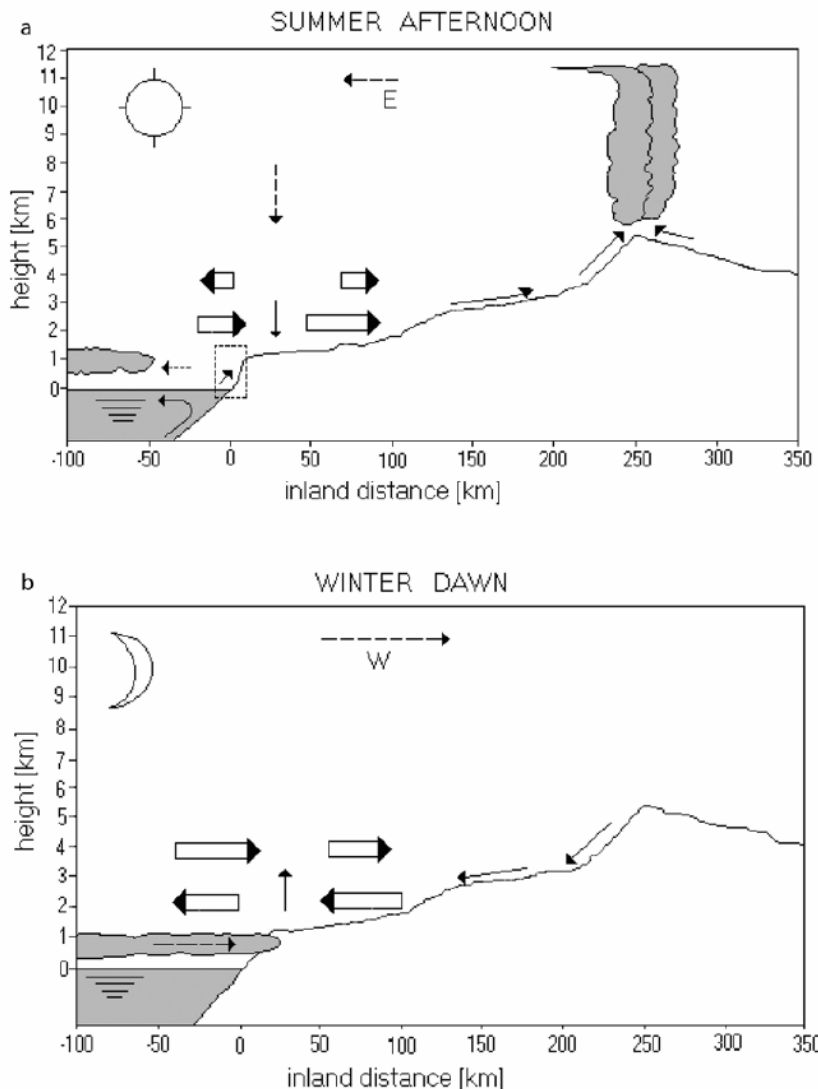
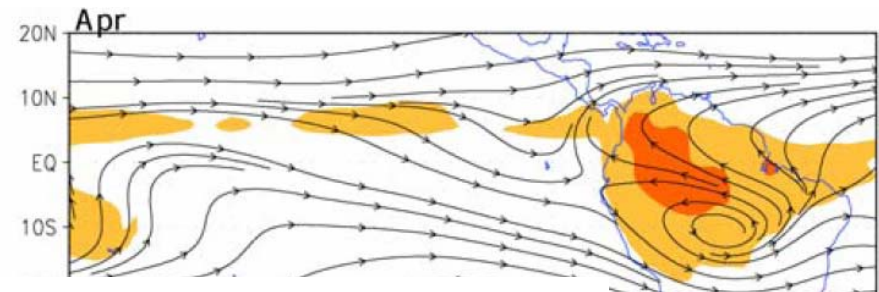
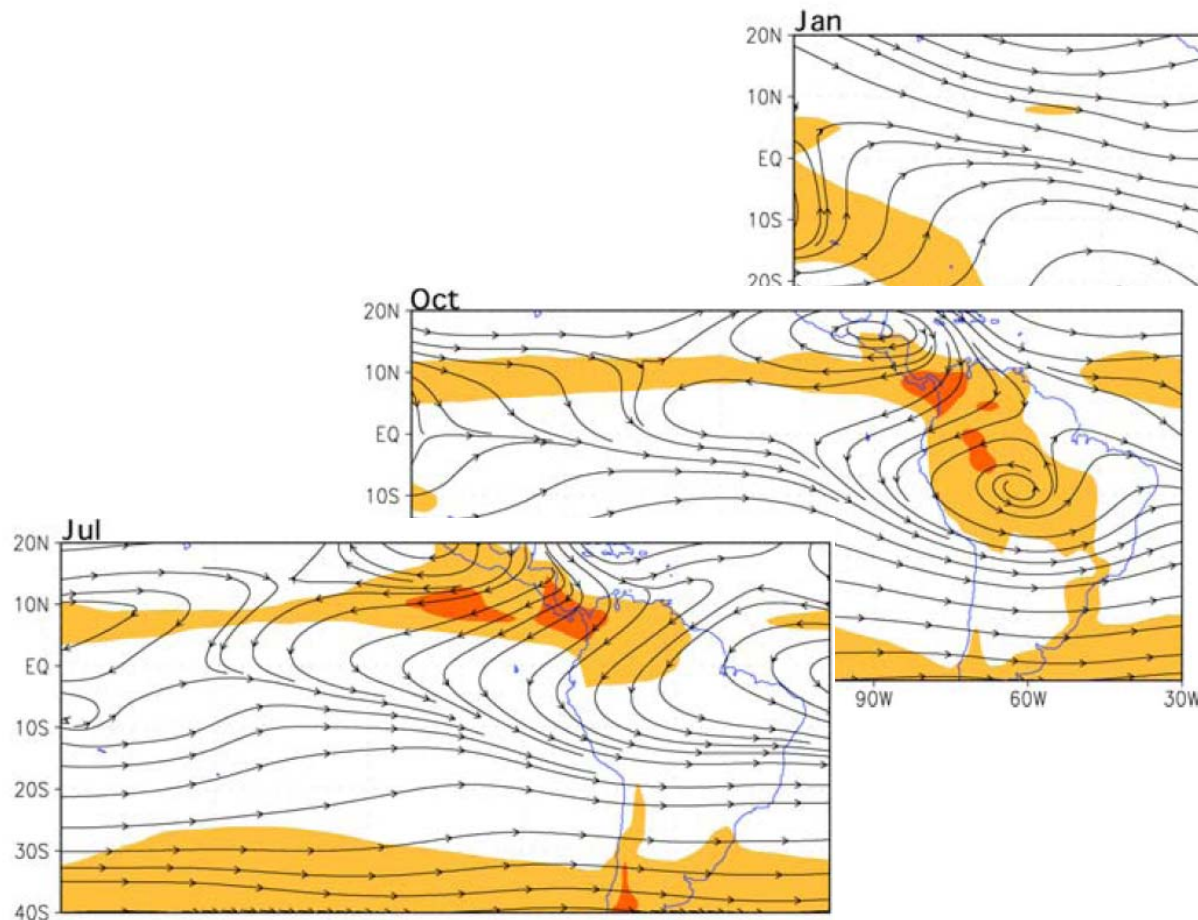


Figure 9. Schematic diagrams of the zonal mass flux (thick arrows) and zonal flow (thin arrows) across the arid northern coast of Chile: (a) austral summer afternoon conditions and (b) austral winter early morning conditions. The dashed rectangle in Figure 9a represents the cross section depicted in Figure 8.

South America monsoonal regime and Altiplano rainfall

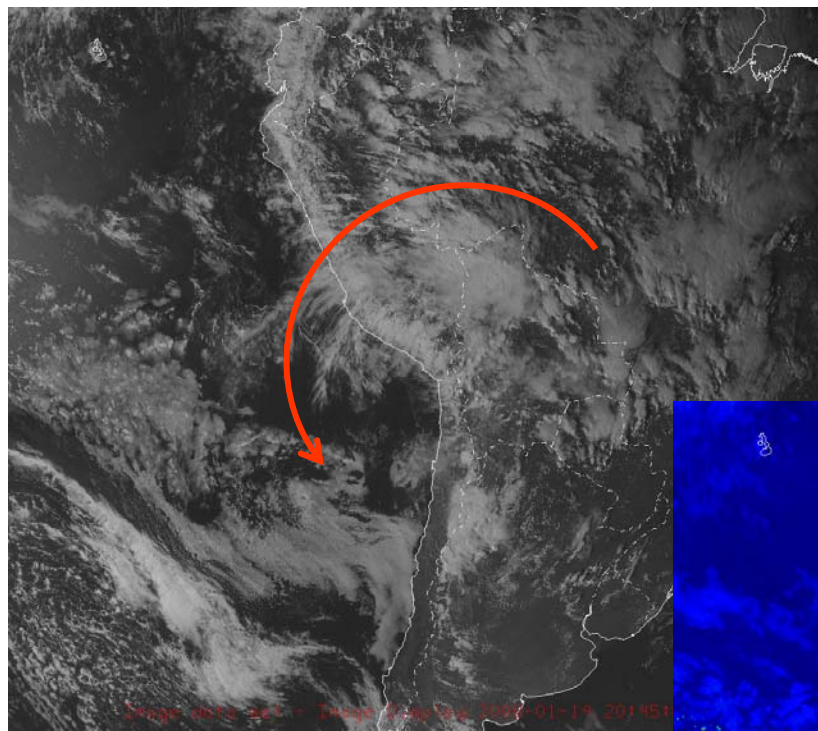
Mean annual cycle

Colors: OLR (proxy of precipitation)
Streamlines: 200 hPa (~12 km) wind

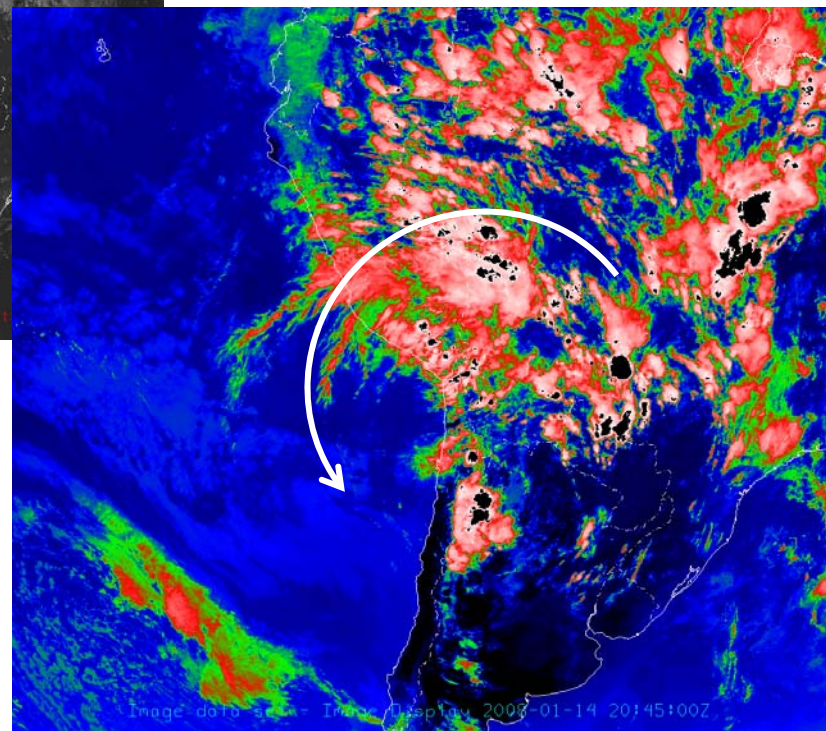


Bolivian High

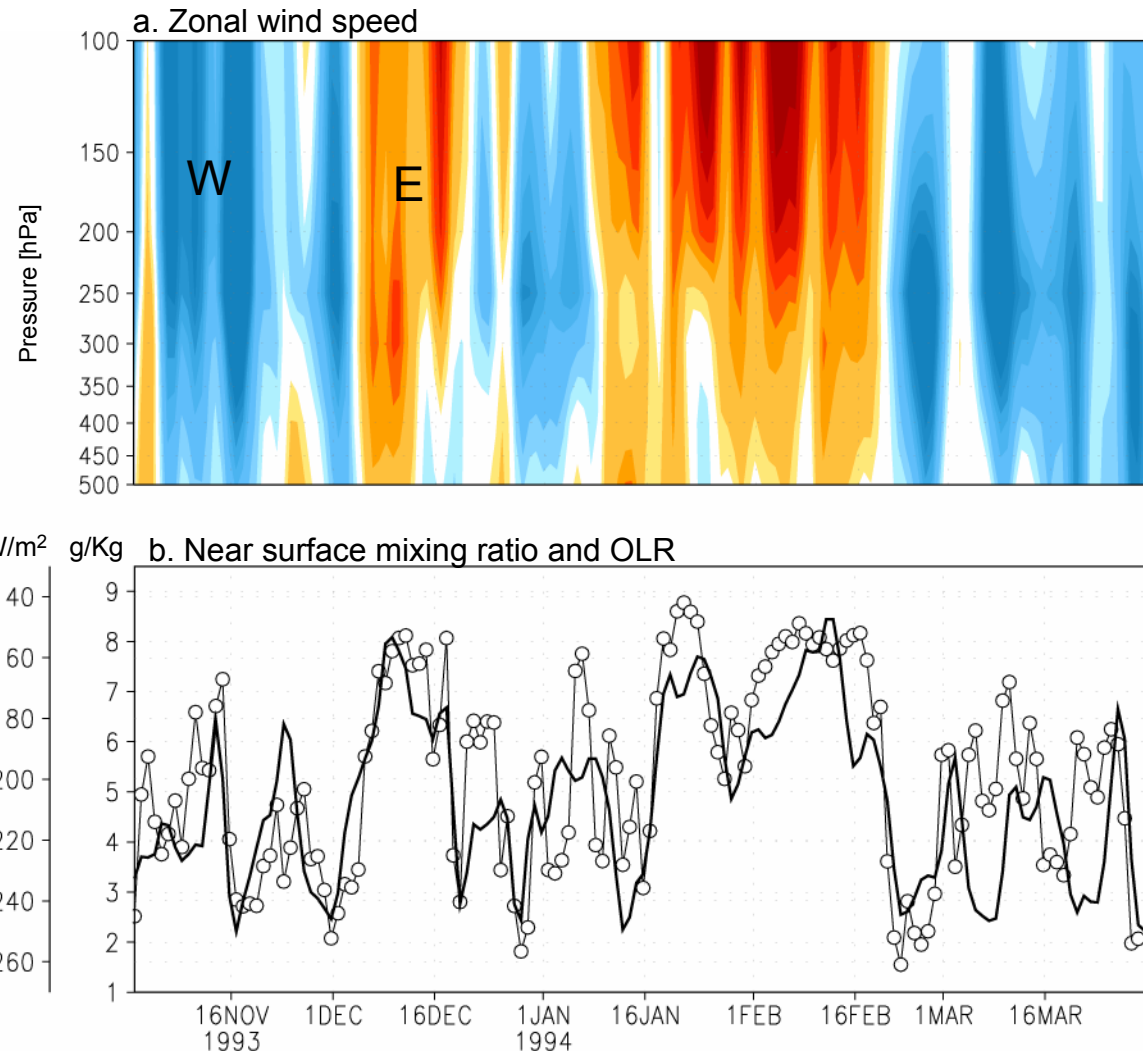
South America monsoonal regime and Altiplano rainfall



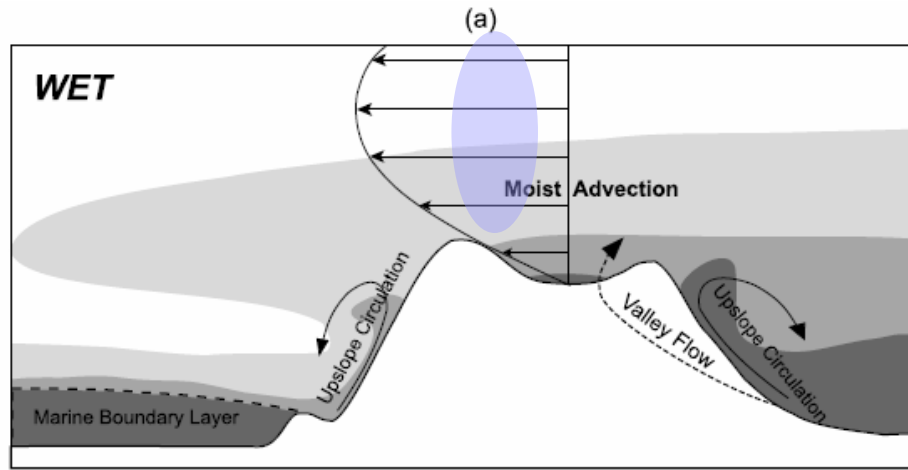
VIS and IR2 GOES images
during an active summer afternoon



Summer Altiplano rainfall: Intraseasonal variability



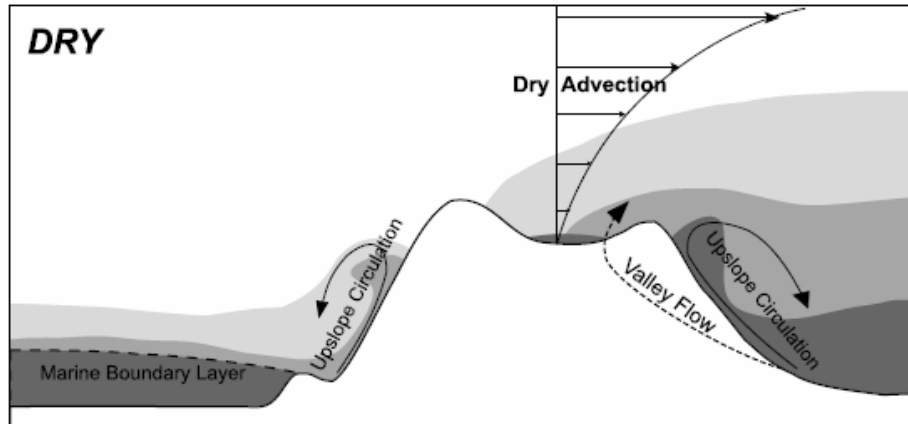
Summer Altiplano rainfall: Intraseasonal variability



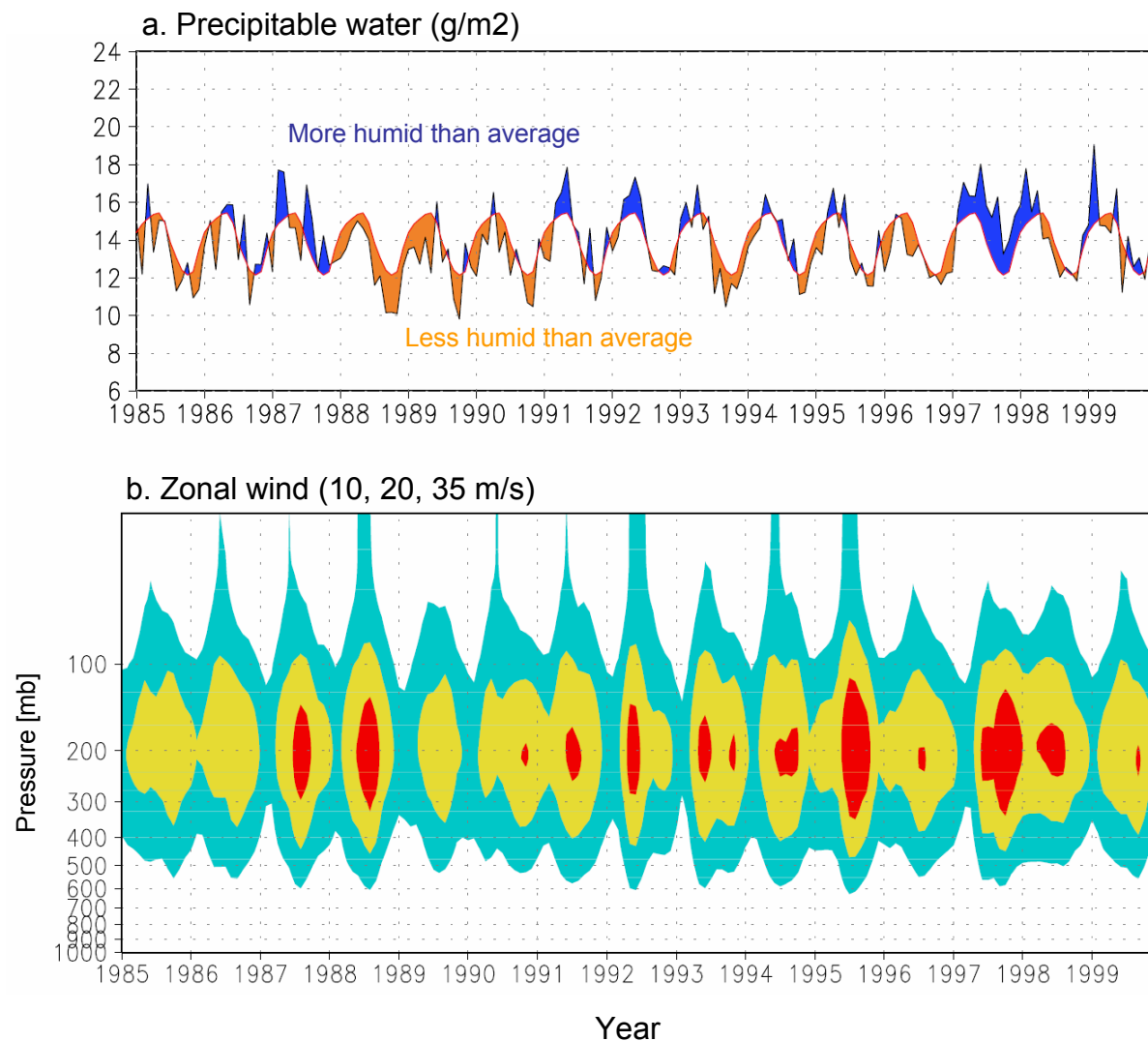
Specific Humidity Color Scale



(b)



Interannual variability of wind and moisture at 30°S-70°W



Interannual variability ~ changes in large-scale circulation

1. Introduction

The climate dynamics literature abounds with patterns of variability; some labeled as teleconnection patterns, oscillations, clusters, seesaws, or modes; many others known only by mode number. The documentation of structures in sea level pressure (SLP) and upper-tropospheric geopotential height fields has proceeded largely independently, each yielding its own set of patterns.

The different analysis techniques used in climate dynamics research also yield different patterns, and even the same technique can yield quite different results, depending upon whether it is applied to a total field or to the zonally symmetric or asymmetric components of that field. The patterns that have emerged in various studies have also been conditioned by the spatial domain of the analysis, the manner in which seasonality is treated, and the time interval over which the data are averaged before the analysis is performed.

Leadings modes of interannual (and longer) of atmospheric variability: ENSO – PDO(?) - AAO

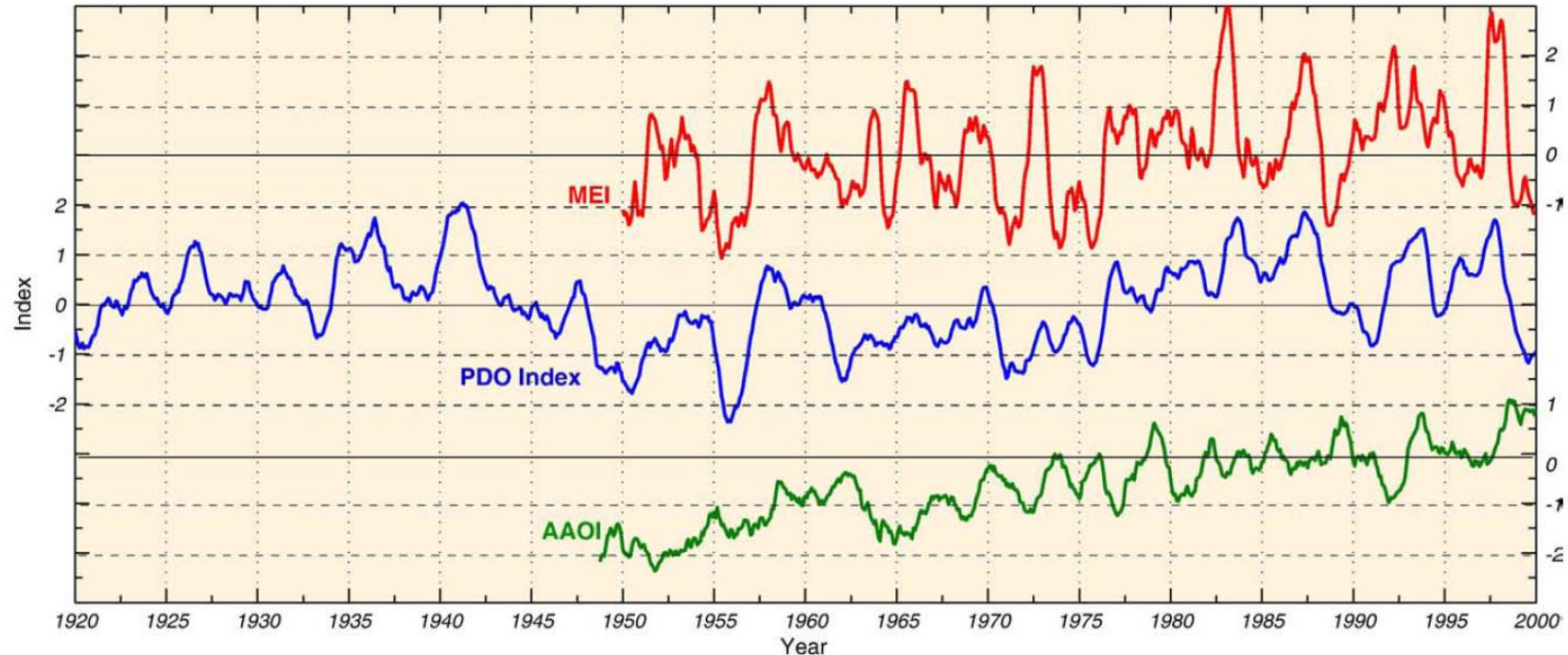
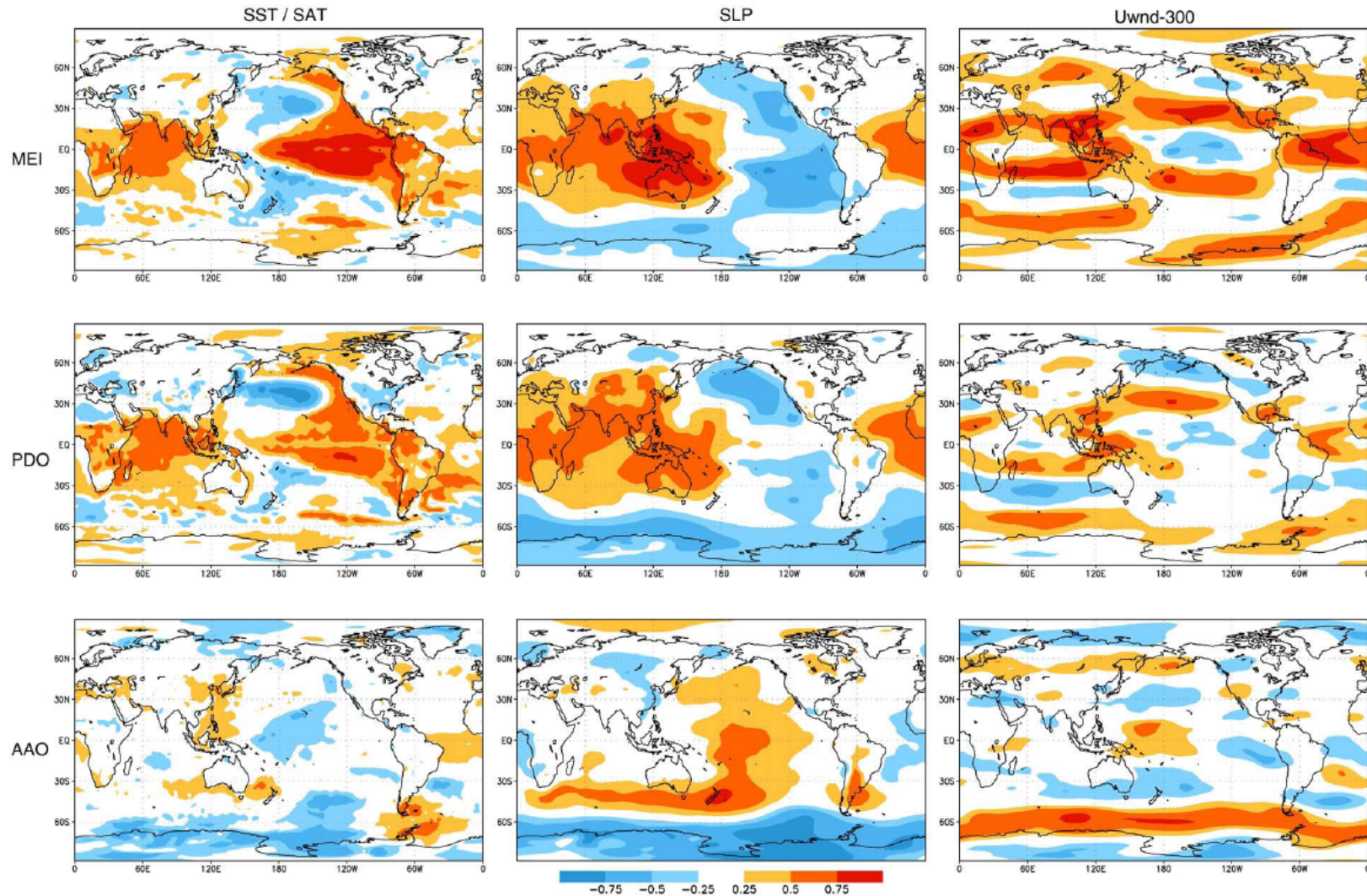
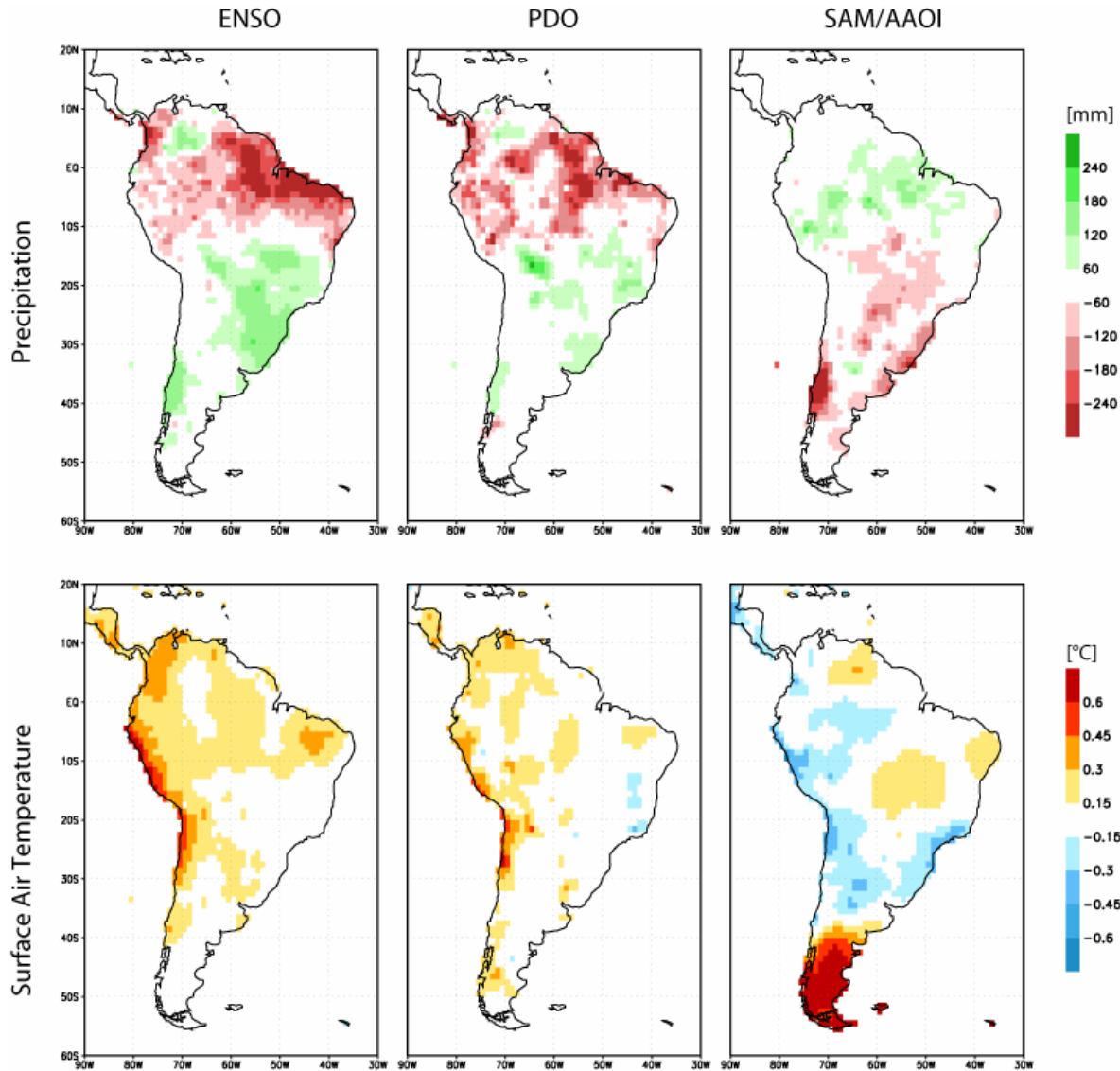


Fig. 5. Time series (1920–2000) of monthly mean Multivariate ENSO Index (MEI), PDO Index and AAO Index. All indexes were smoothed using a 5-month running mean filter. Original indices obtained from Climate Diagnostic Center (NOAA).

Leadings modes of interannual (and longer) of atmospheric variability: ENSO – PDO(?) - AAO



Annual mean Precip/SAT regressed upon index of large-scale modes (50 years of data)



Interannual variability

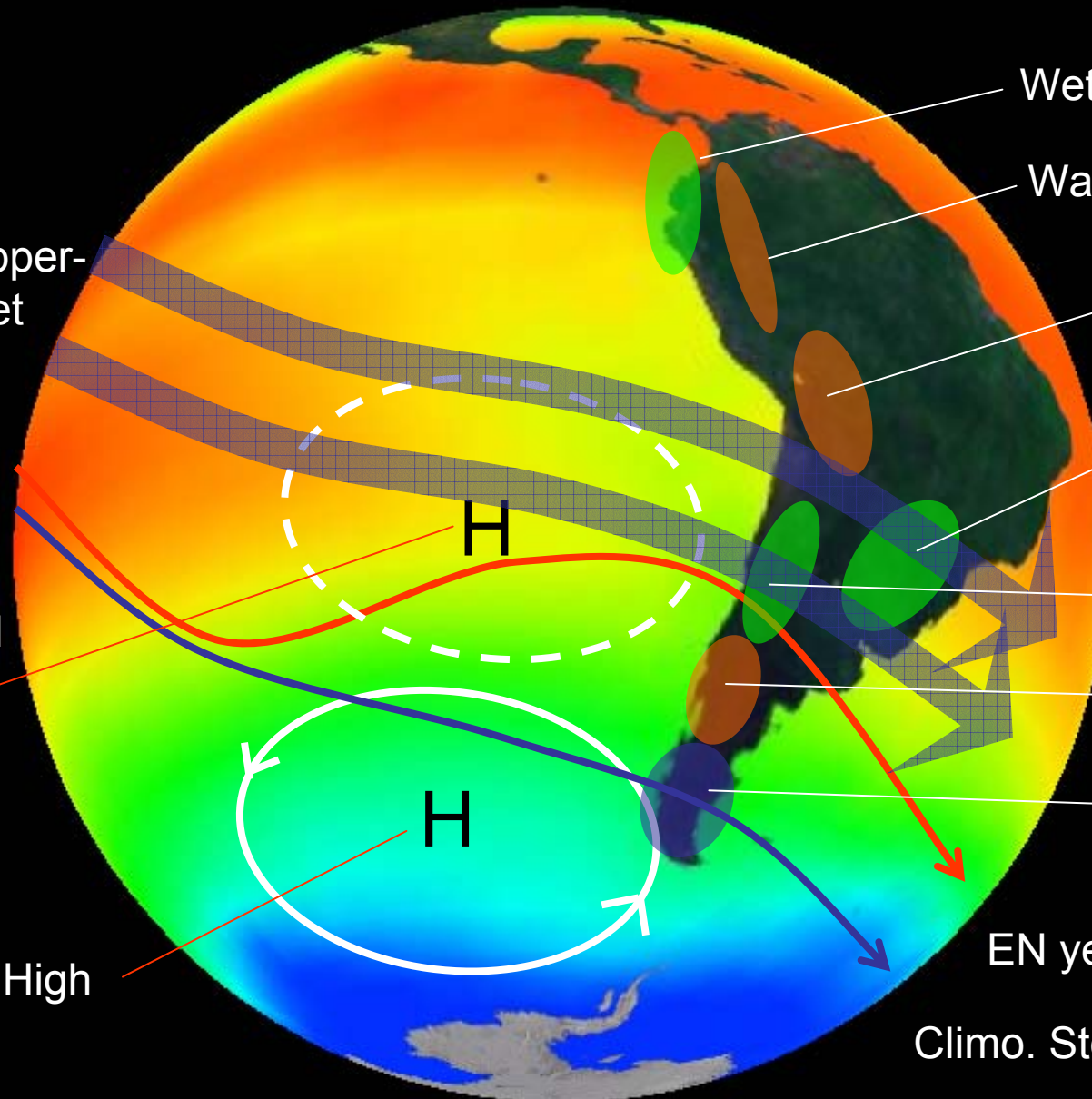
-

Major ENSO impacts

Stronger upper-
Level ST Jet

Weakened
ST High

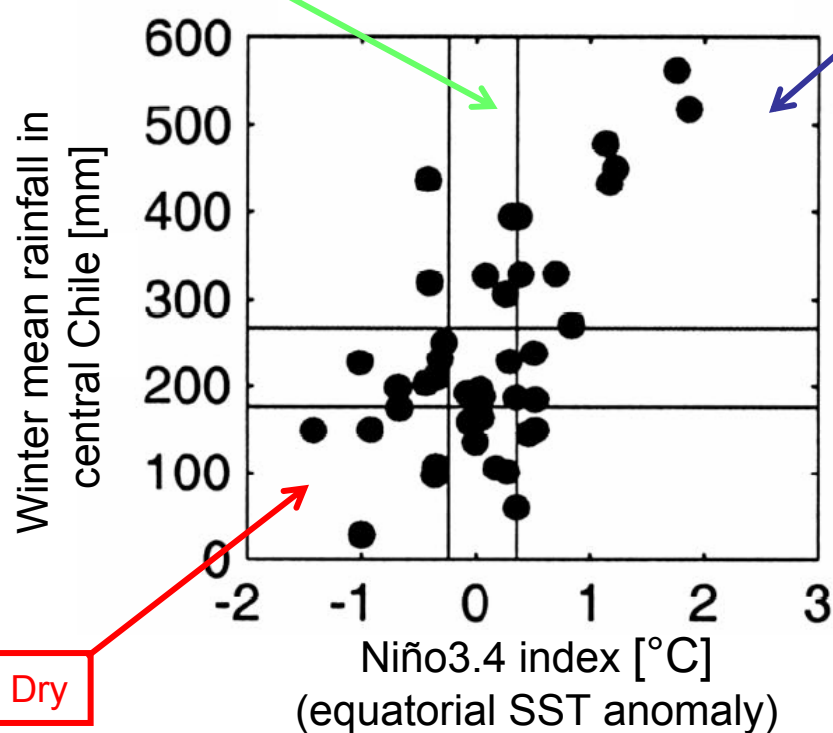
Blocking High



EN years Storm Track

Climo. Storm Track

Variabilidad interanual de la precipitación de invierno en Chile central



Montecinos & Aceituno 2001

ENSO-related variability explains about 1/3 of the central Chile rainfall variability. Not quite enough for seasonal prediction...look for other forcing

Summer Altiplano rainfall: Interannual variability

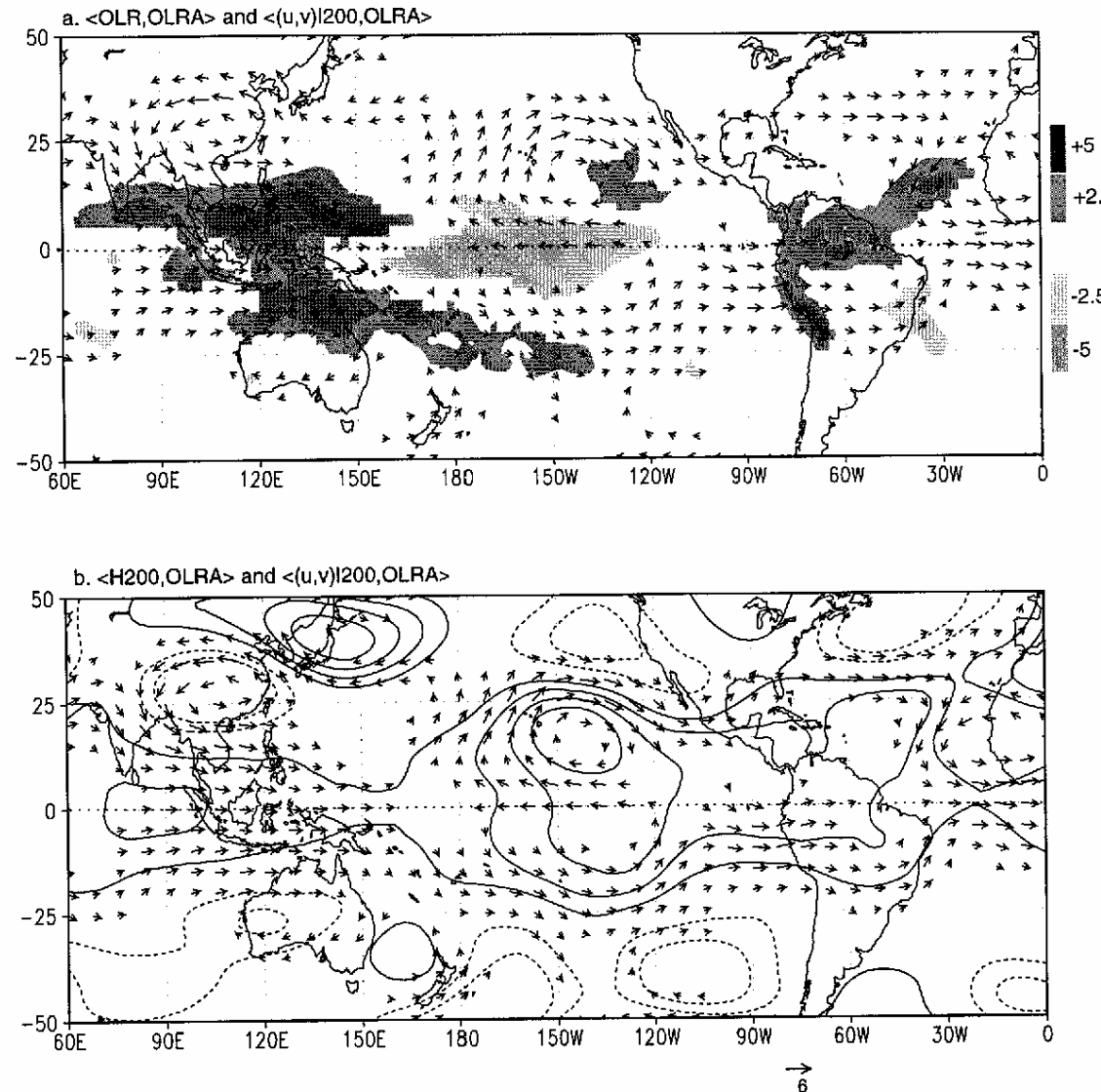
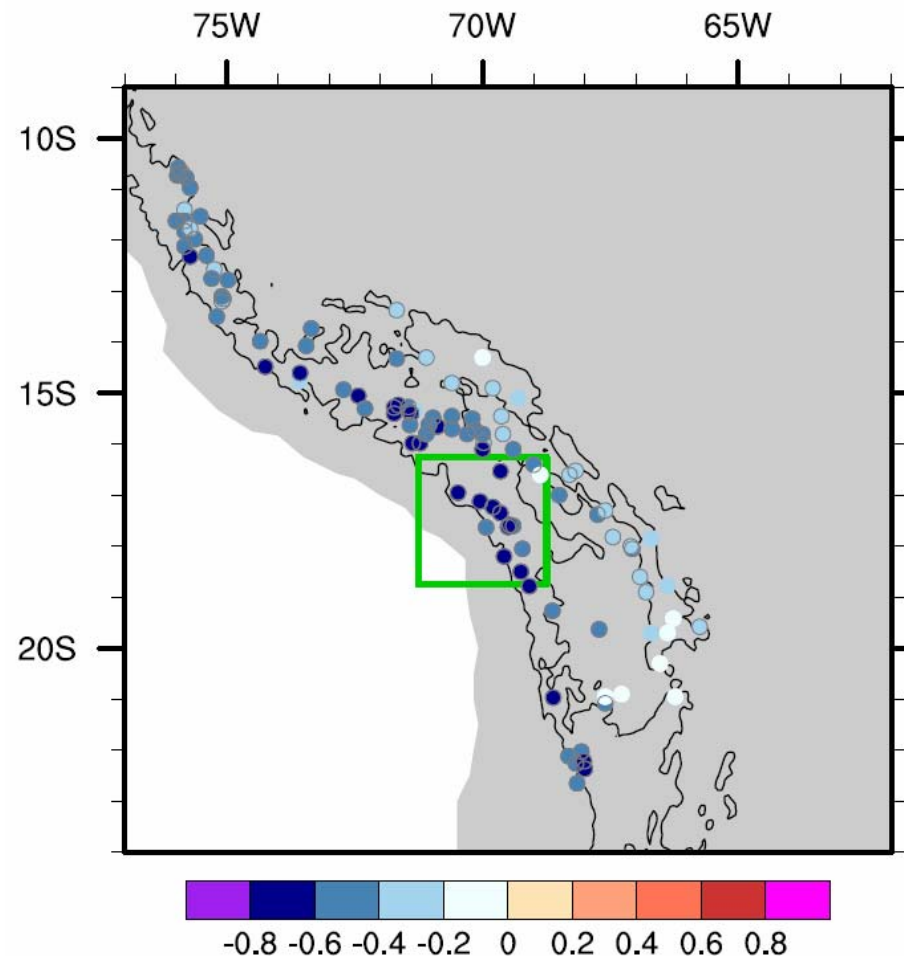


FIG. 7. Regression maps in the interannual range (see section 2 for details on calculation and statistical significance). (a) OLR (shaded, scale in units of W m^{-2} per std dev) and 200-hPa wind regressed upon CI (OLR over the Altiplano). (b) 200-hPa height and winds regressed upon CI. Contour interval is 30 m per std dev. Negative values in dashed line. The zero contour is omitted. Only values and wind vectors statistically significant at the 95% confidence level are shown. Reference wind vector (in m s^{-1}) at the bottom of the figure.

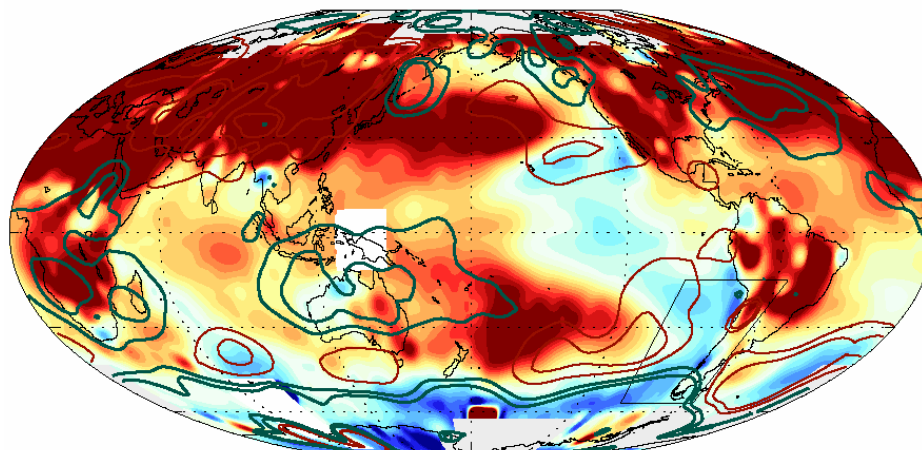
Summer Altiplano rainfall: Interannual variability

Correlation between DJF precipitation and U200 (17S-70W)

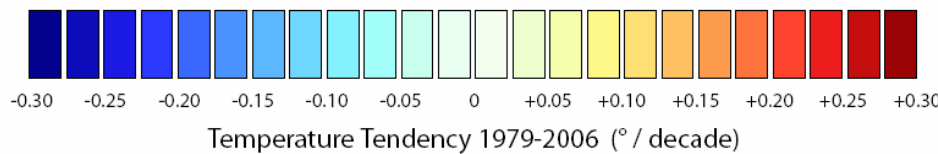
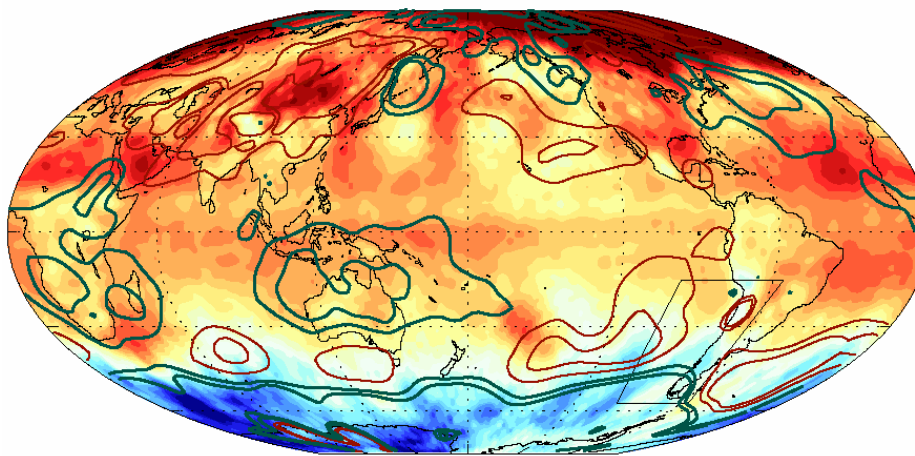


Observed trends (last 3 decades): Air temperature

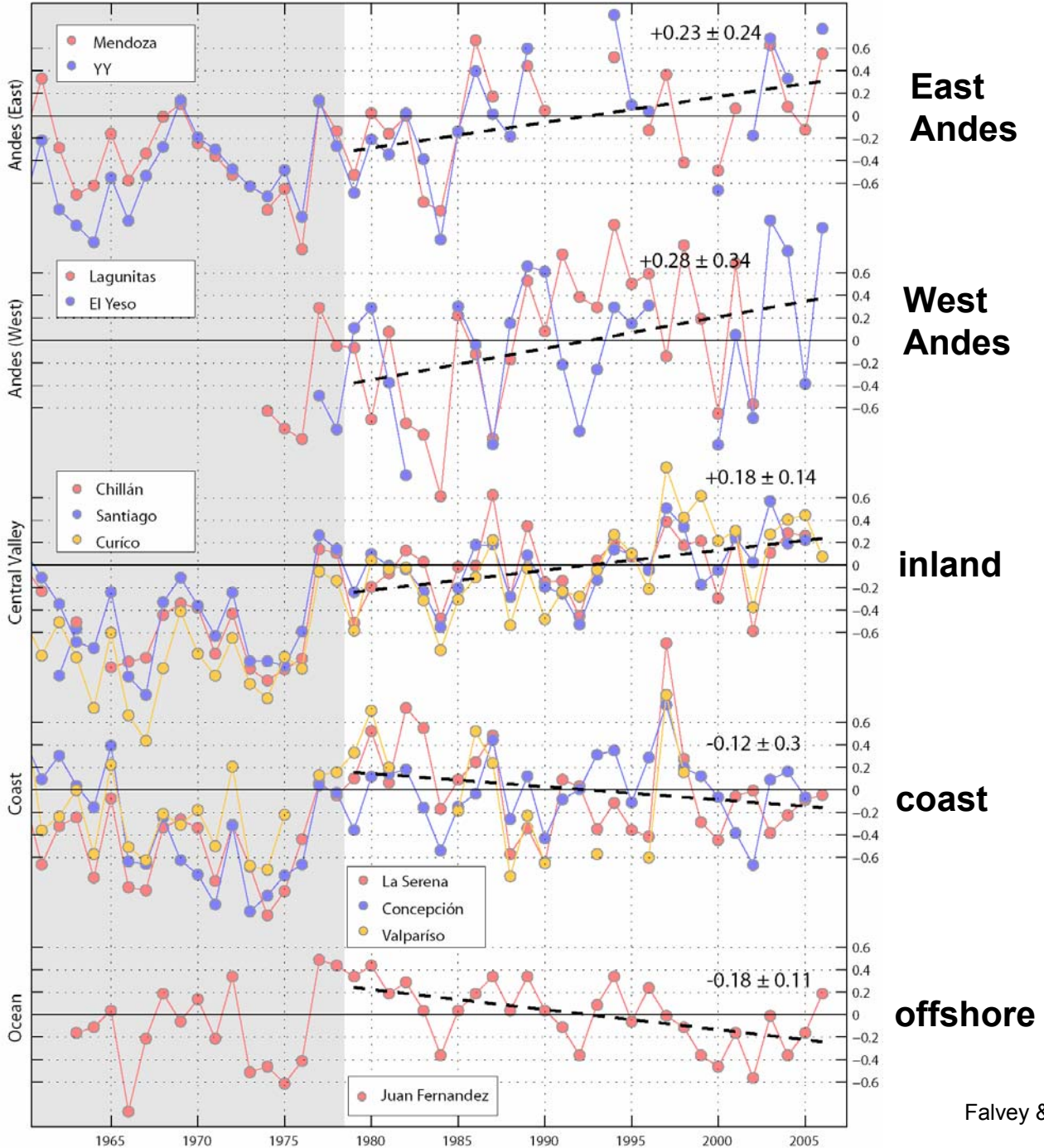
Surface Air Temperature and SST (NCDC)



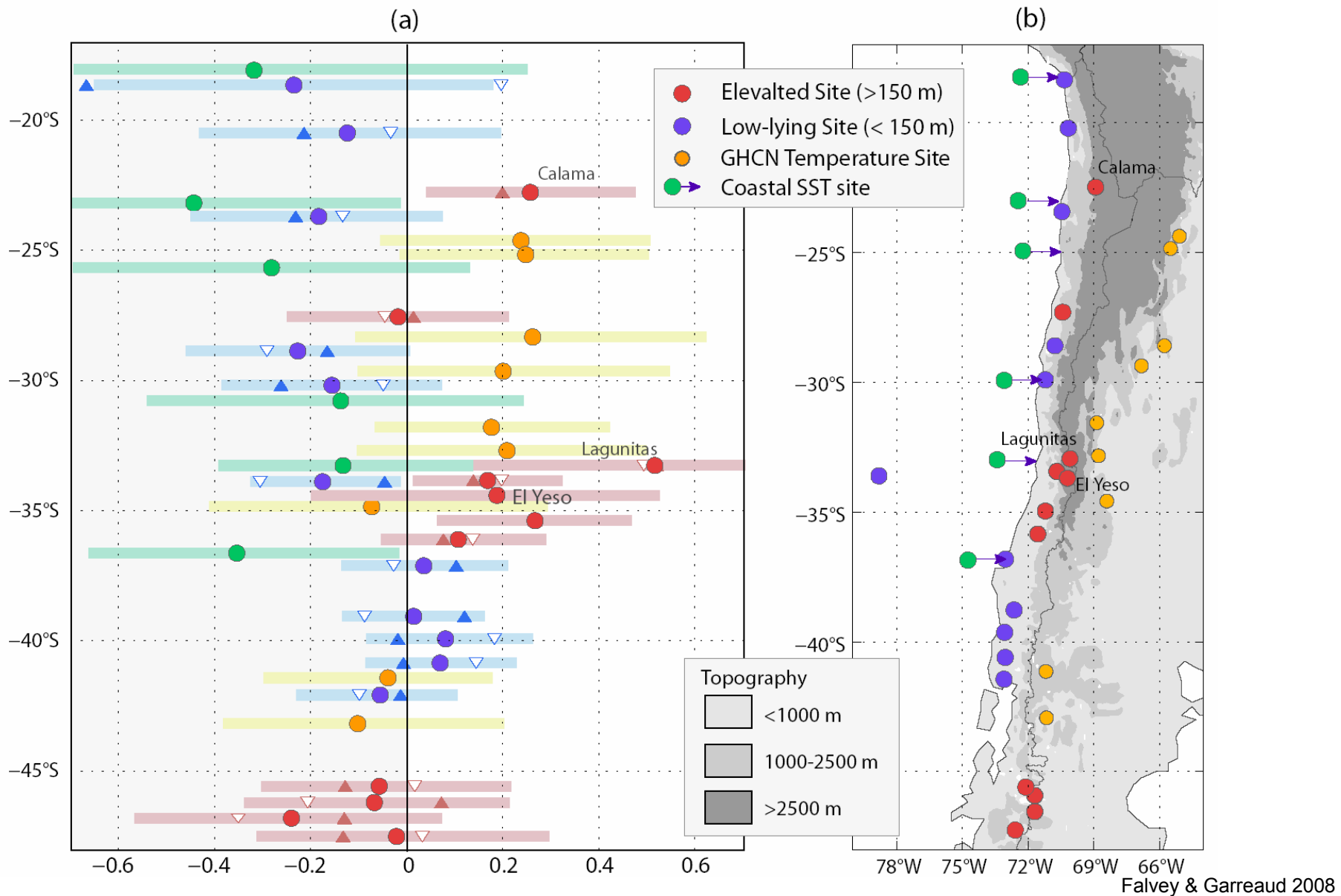
Mid-Troposphere Air Temperature (MSU)



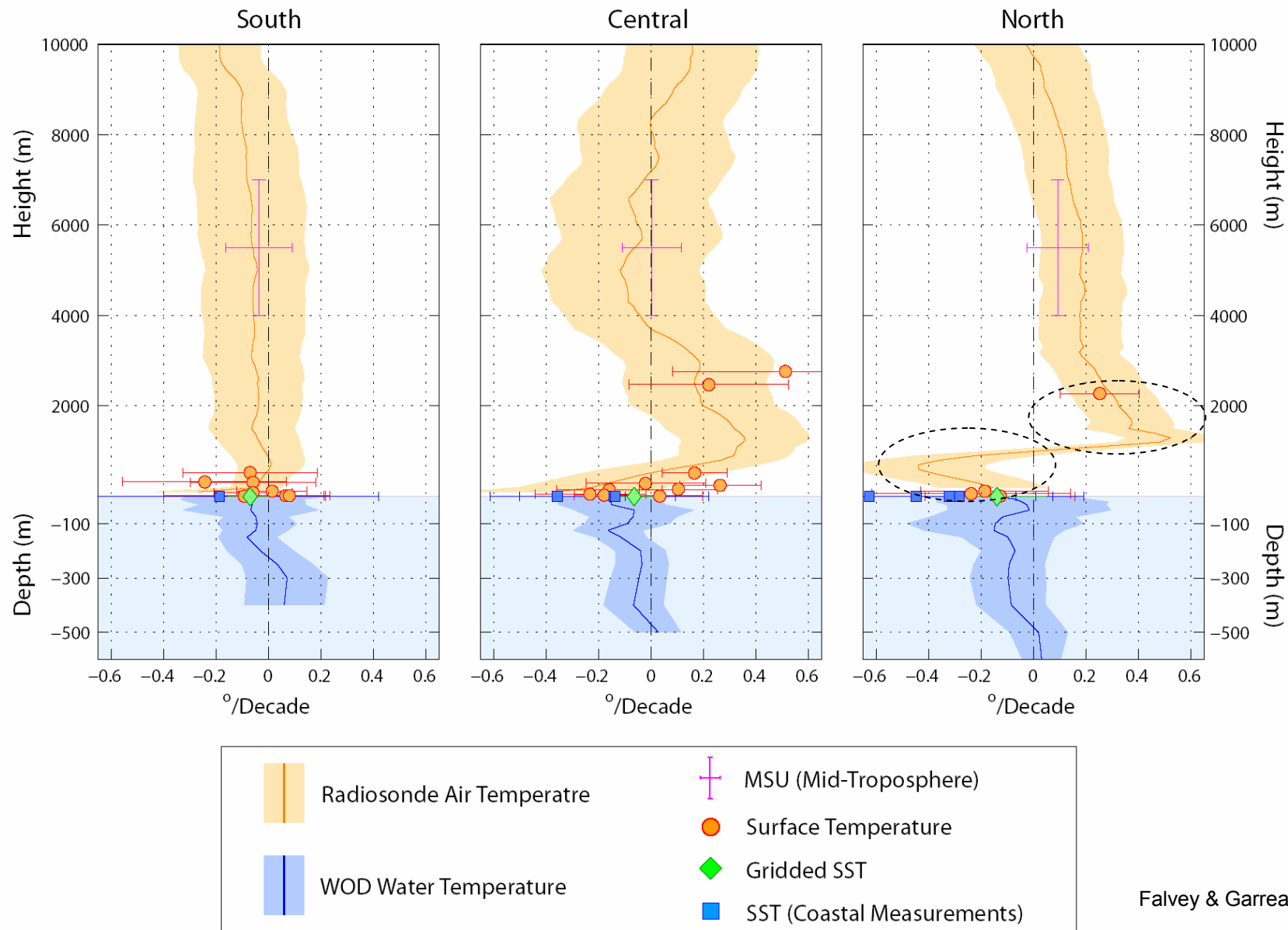
Observed trends (last 50 years): SAT



Ocean cooling – land warming along north-central Chile. Pattern reverses farther south



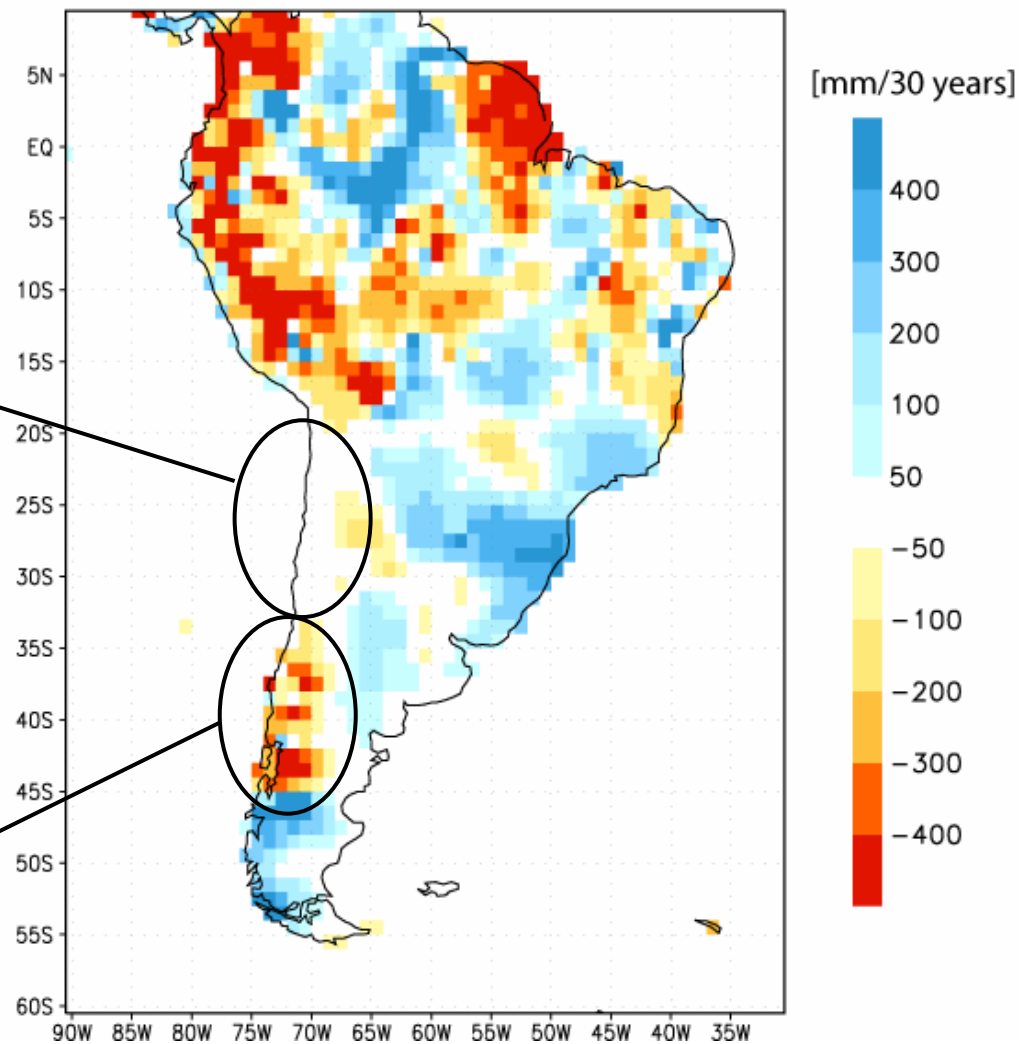
Cooling MBL / warming lower free troposphere → increased lower tropospheric stability Sc?



Observed trends: Precipitation 1970-2000

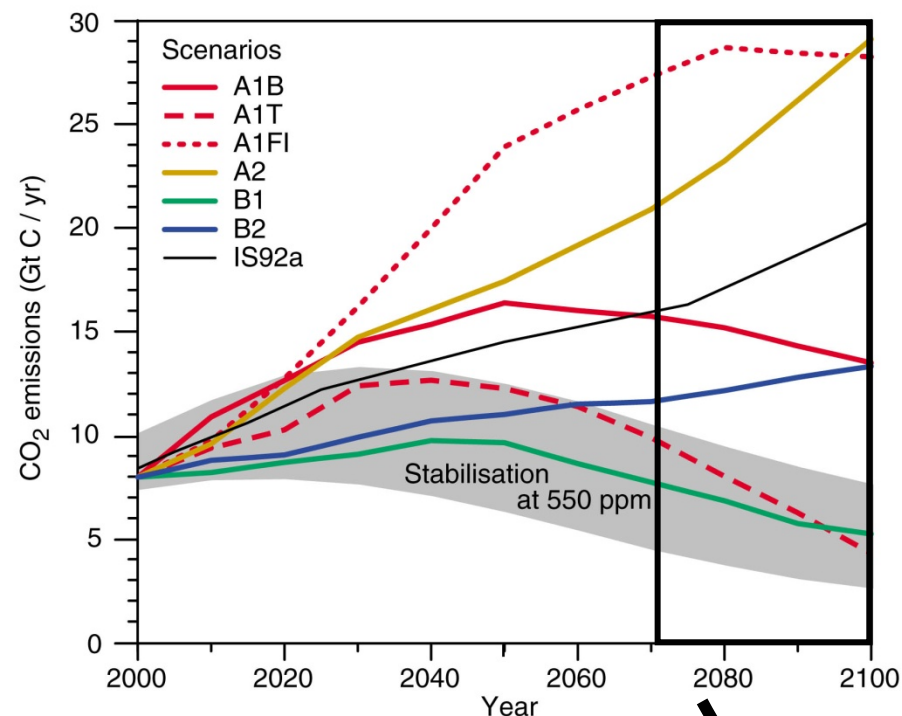
- Semiarid climate
- MAP \sim 30-500 mm
- $\sigma(\text{IA})/\text{MAP} \sim 0.3 - 0.5$
- Strong ENSO Impact
- No significant trend

- Rainy climate
- MAP \sim 1000-3000 mm
- $\sigma(\text{IA})/\text{MAP} \sim 0.1$
- Weak ENSO Impact
- Significant drying trend

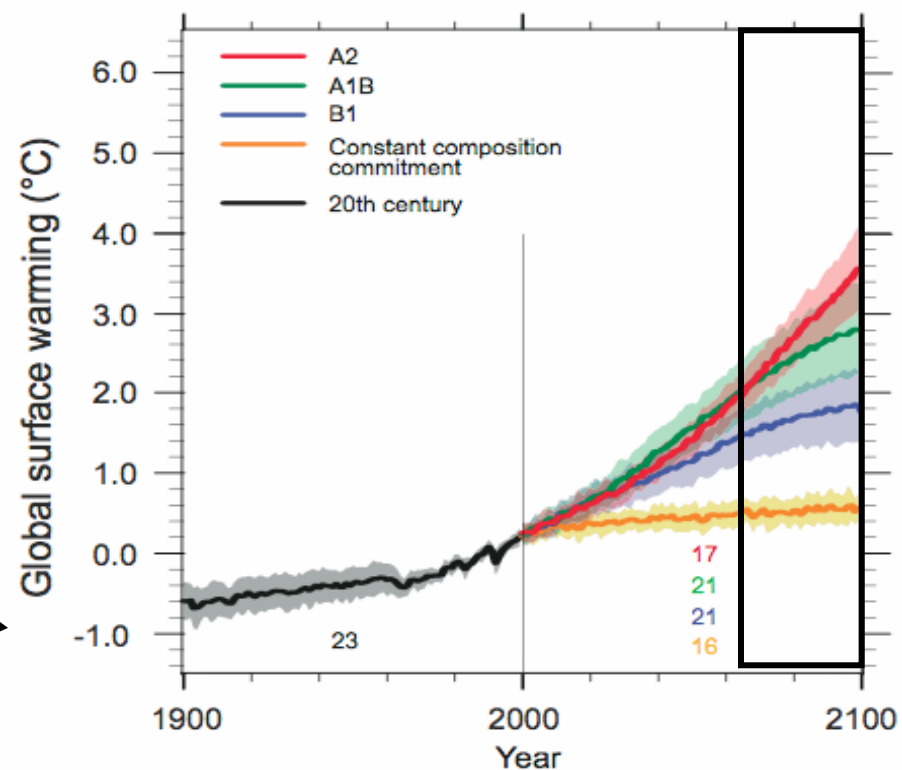


Future Climate Scenarios

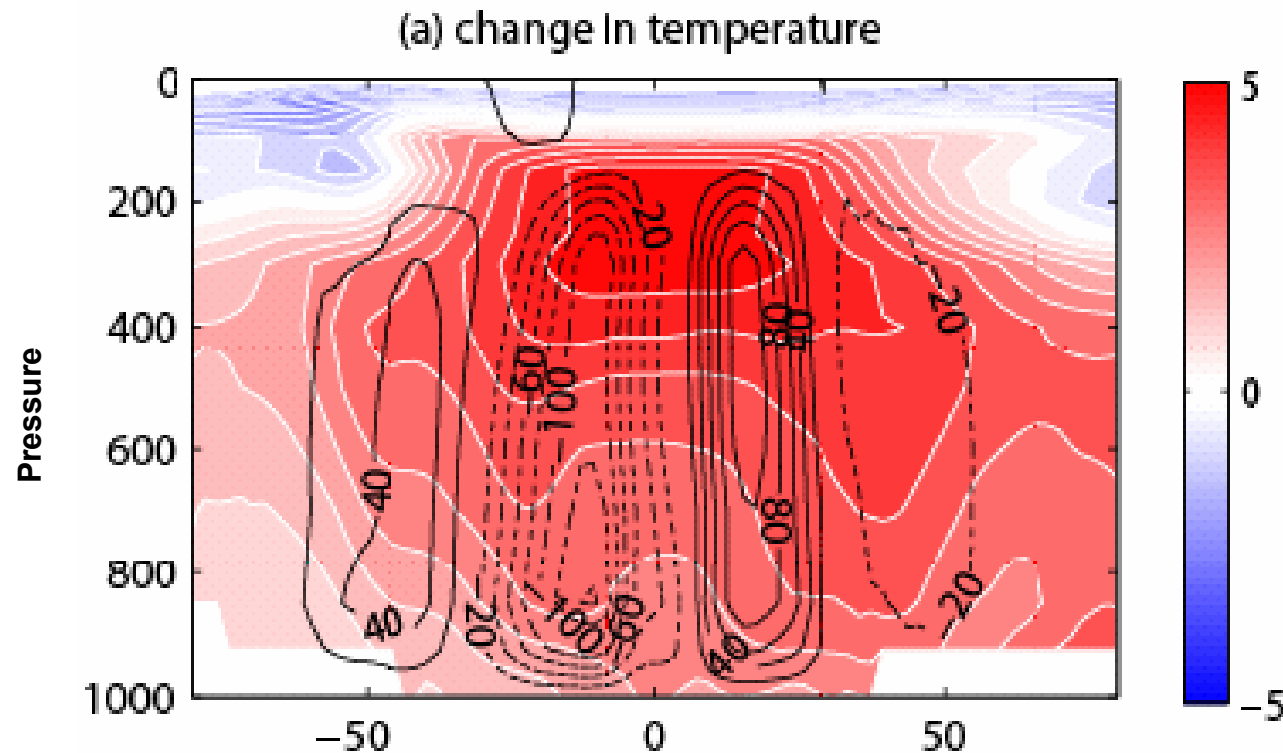
GHG (CO₂,...) emissions projections + GCMs



20+ GCMs
CMIP3/IPCC AR4



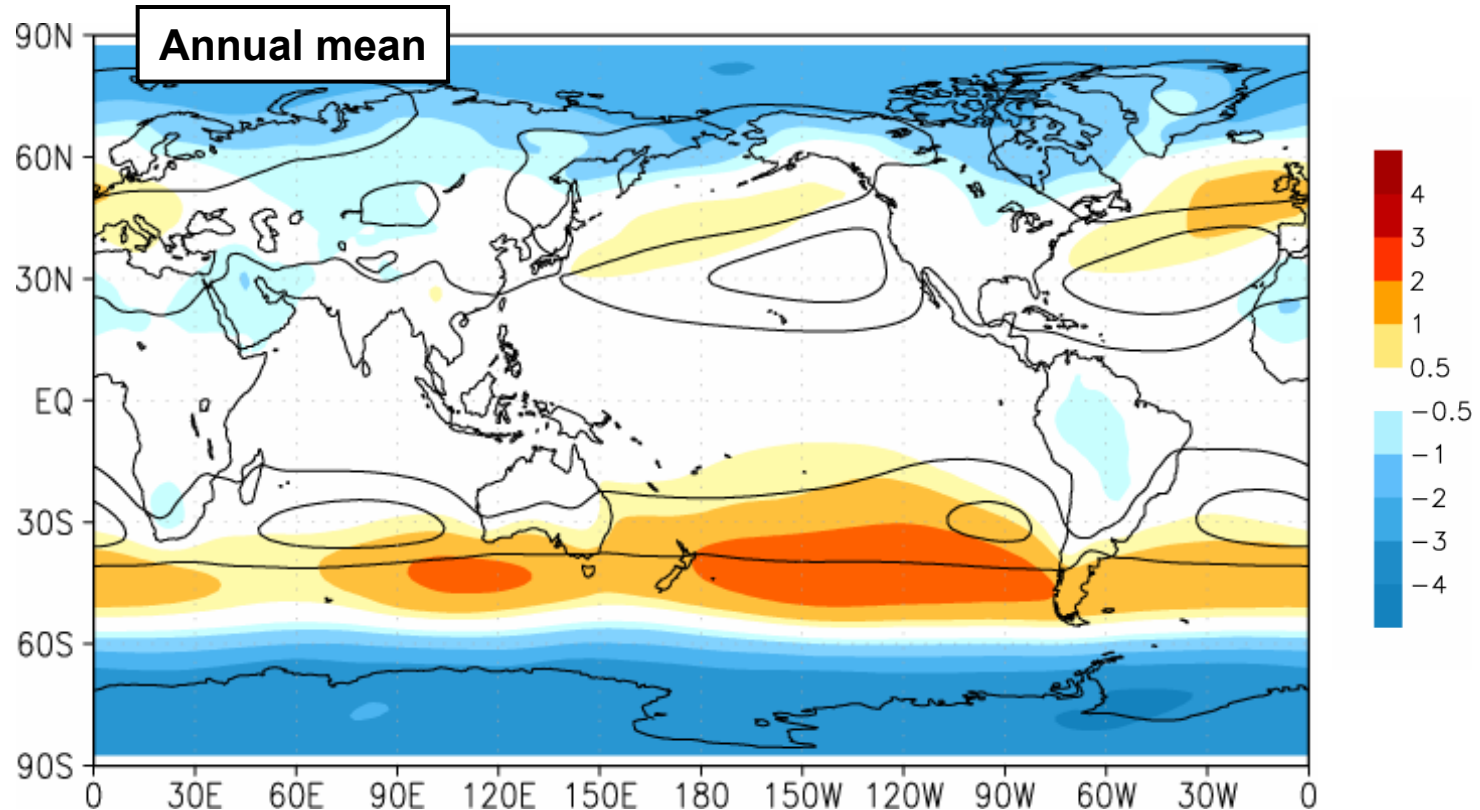
Multimodel average of difference in zonal mean air temperature between A2 and BL



Lu et al. 2007

Warming of the tropical upper troposphere ► Increased static stability at subtropics and midlatitudes ► poleward expansion of the Hadley cell

Multimodel average SLP difference between A2 (2070-2100) and BL (1970-2000)



Strengthening of the poleward flank of subtropical anticyclones and poleward shift of the midlatitude storm track is very consistent among GCMs

Multimodel precipitation and surface temperature Changes (A2-BL)

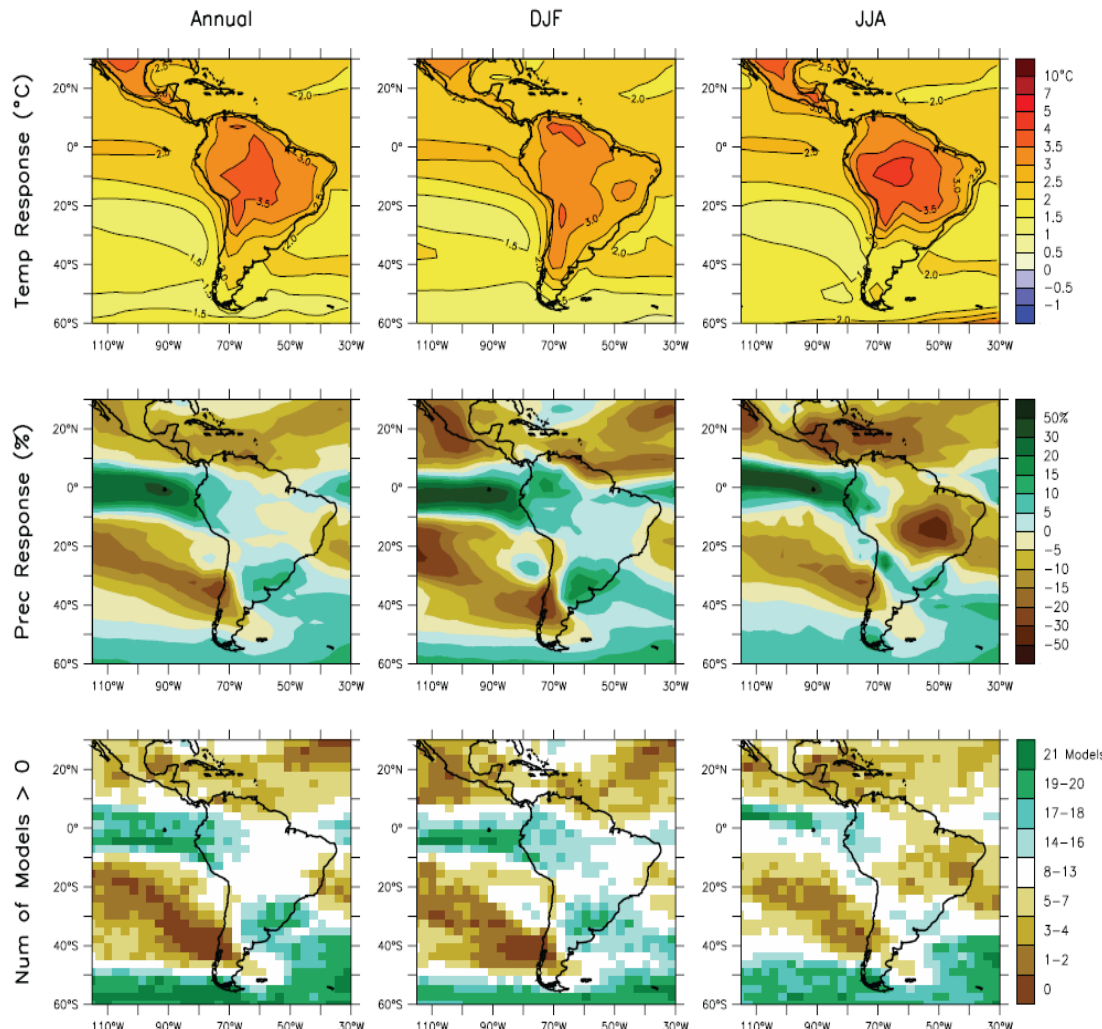
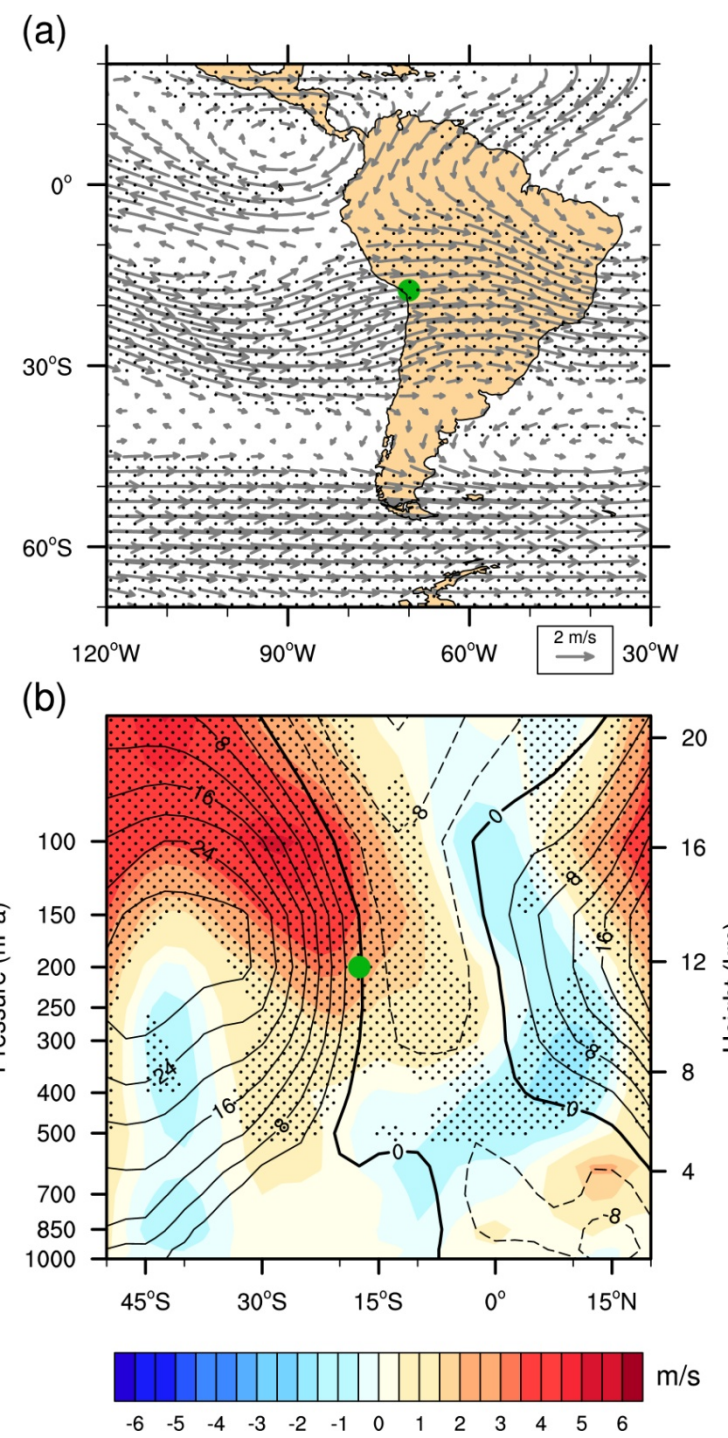


Figure 11.15. Temperature and precipitation changes over Central and South America from the MMD-A1B simulations. Top row: Annual mean, DJF and JJA temperature change between 1980 to 1999 and 2080 to 2099, averaged over 21 models. Middle row: same as top, but for fractional change in precipitation. Bottom row: number of models out of 21 that project increases in precipitation.

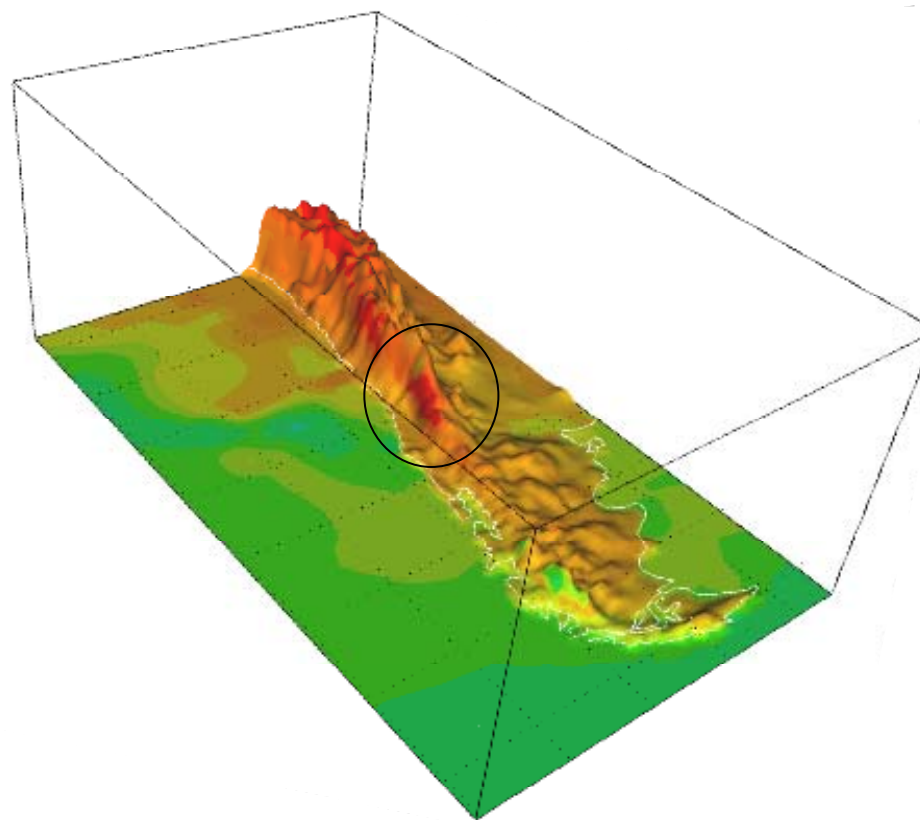
Future Climate Scenarios



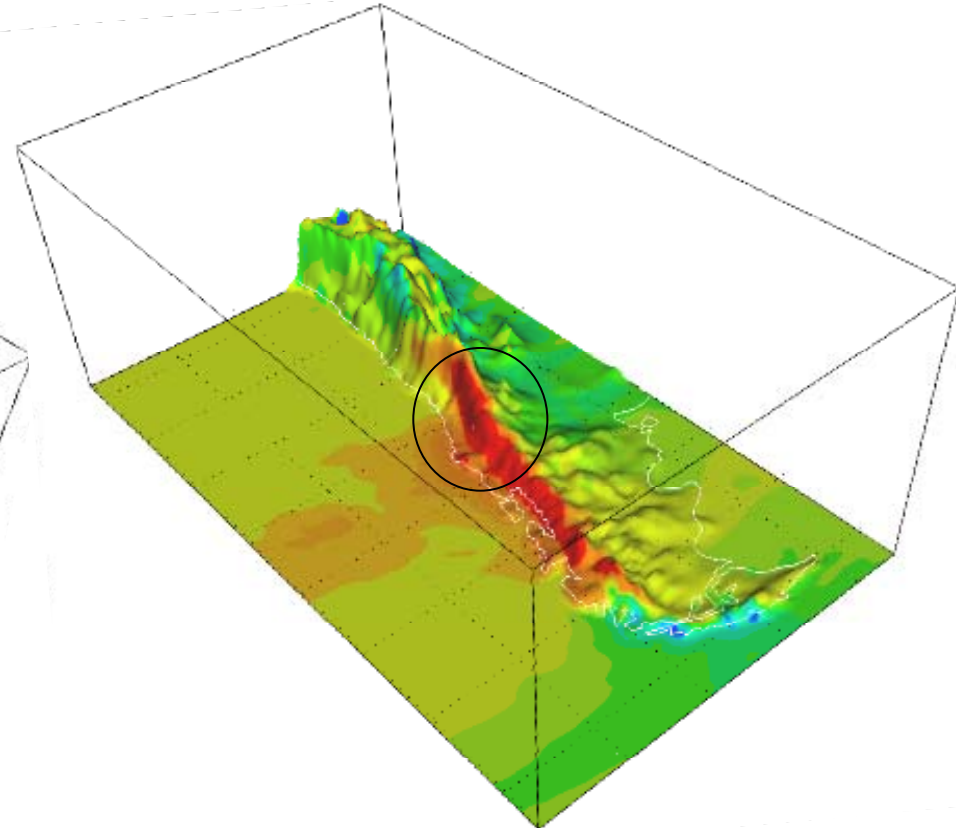
Differences A2(2100-2070) – BL(1960-1990)

Obtained with a regional climate model (PRECIS) forced by HadCM3 / A2

Temperatura Superficial (SAT)

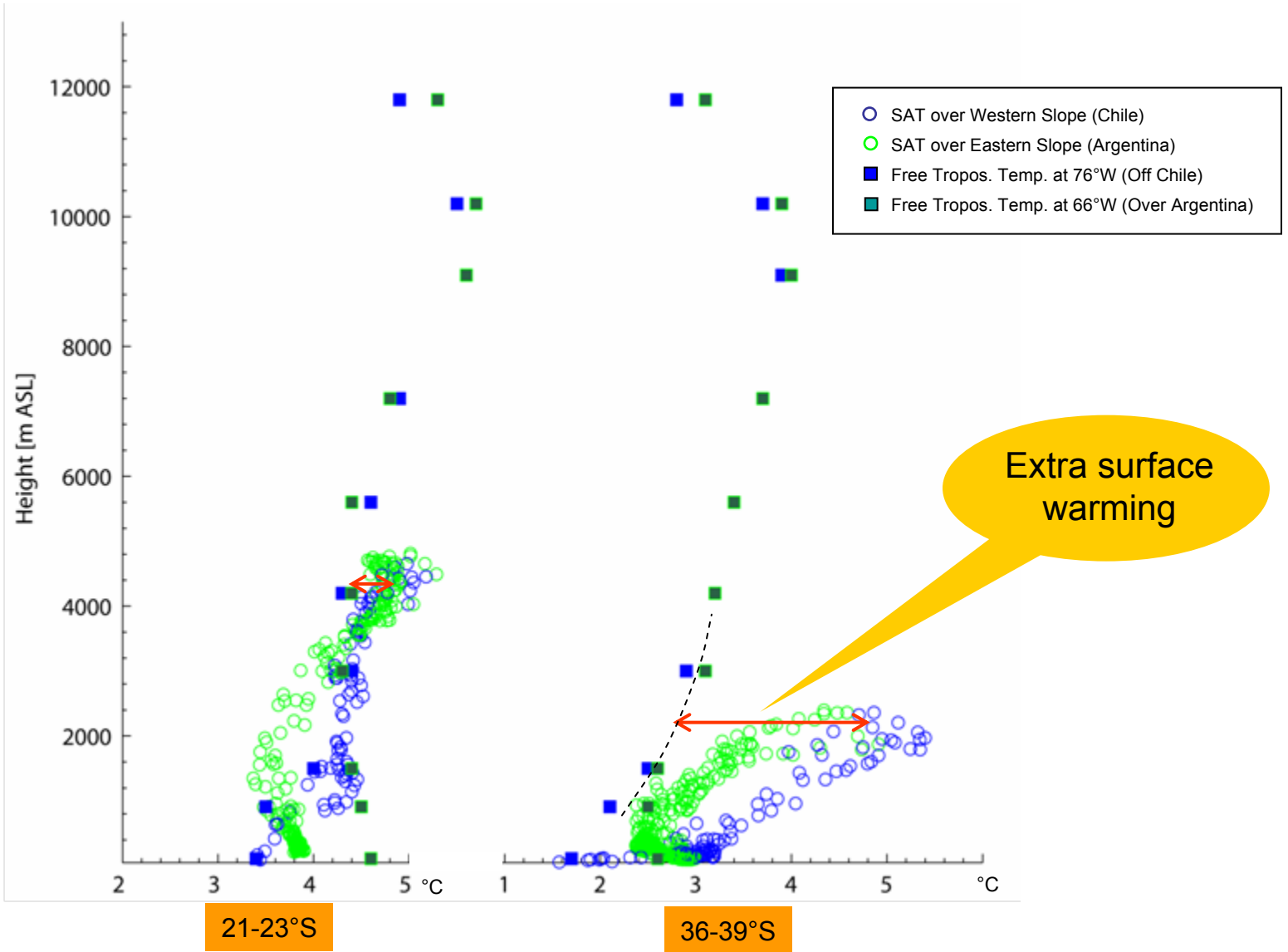


Precipitación (P)

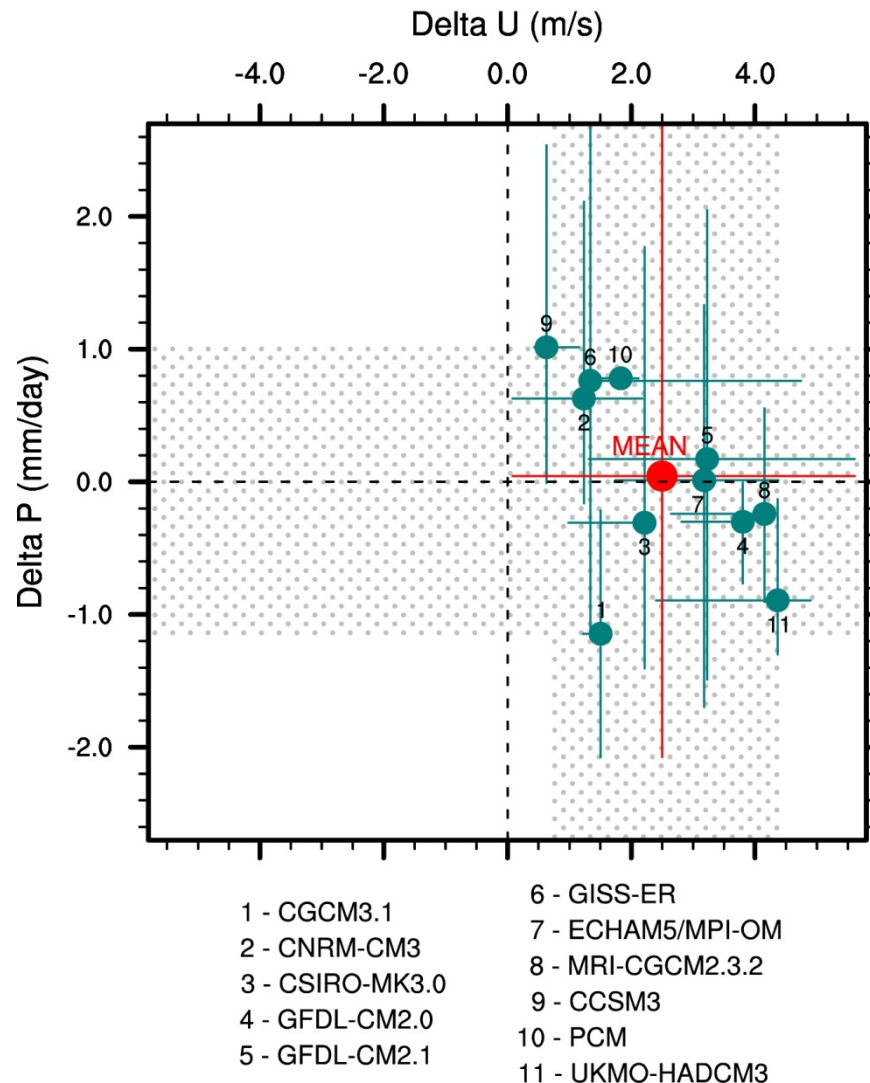


PRECIS-DGF-UCH

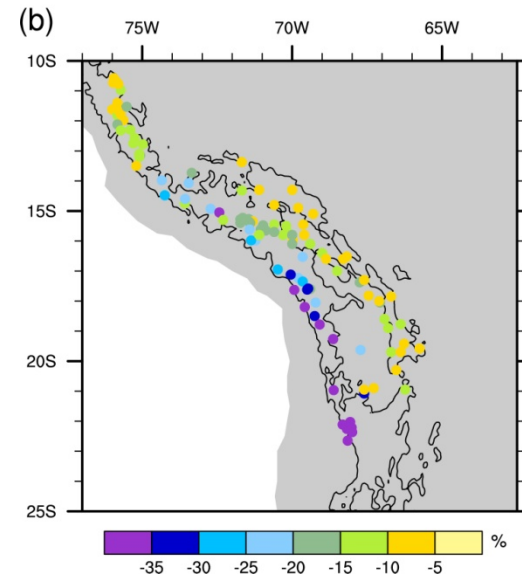
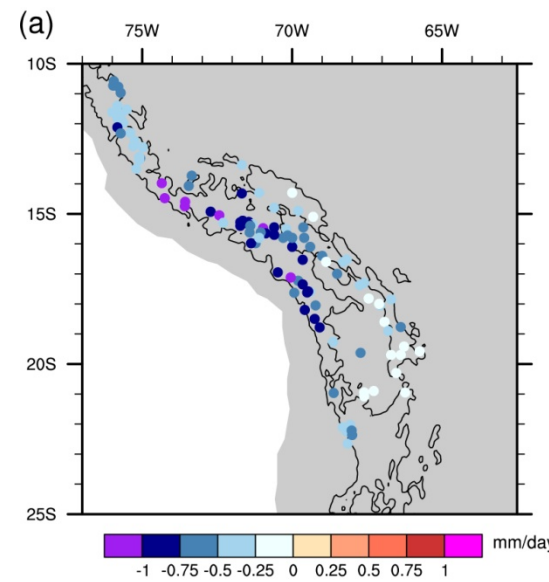
ΔT (A2-BL) versus Height



Precipitation Changes over the Altiplano: ζ ?



Precipitation Changes over the Altiplano: Drier and warmer



Material Adicional....

Atmospheric circulation is governed by fluid dynamics equation + ideal gas thermodynamics

$$\frac{d\vec{V}}{dt} + f\hat{k} \times \vec{V} = -\frac{1}{\rho} \nabla p - \vec{F}_r + \vec{g}$$

Momentum eqn.

$$(\frac{\partial}{\partial t} + \vec{V} \cdot \nabla) T - S_p \omega = Q_{RAD} + Q_{Conv} + Q_{Sfc}$$

Energy eqn.

$$\nabla \cdot \vec{V} + \frac{\partial \omega}{\partial p} = 0$$

Mass eqn.

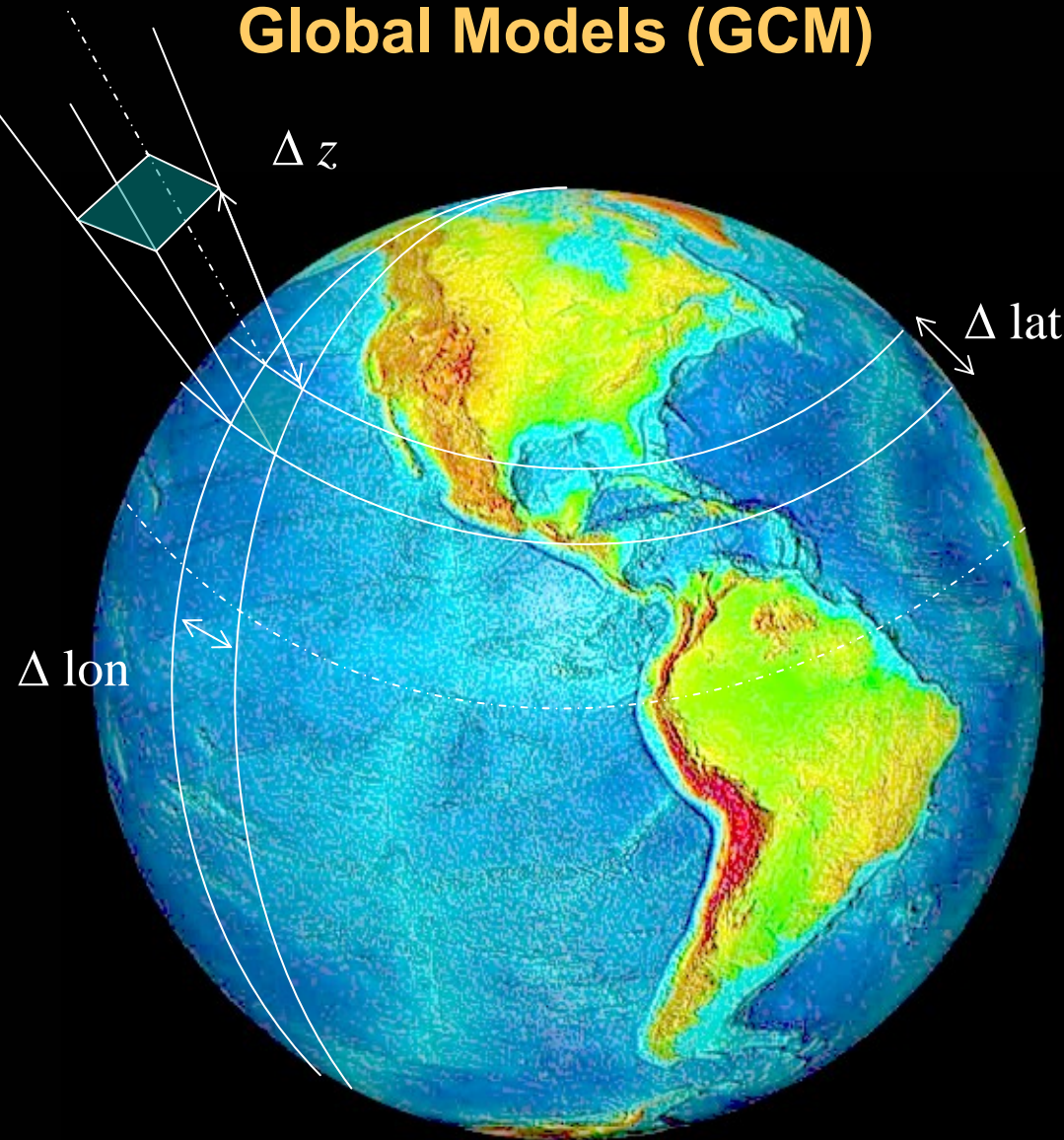
$$\frac{\partial(gz)}{\partial p} = -\frac{RT}{p}$$

Idea gas law

$$\frac{dq_v}{dt} = -C + E$$
$$\frac{dq_r}{dt} = +C - E + S_r$$

Water substance eqns.

Global Models (GCM)



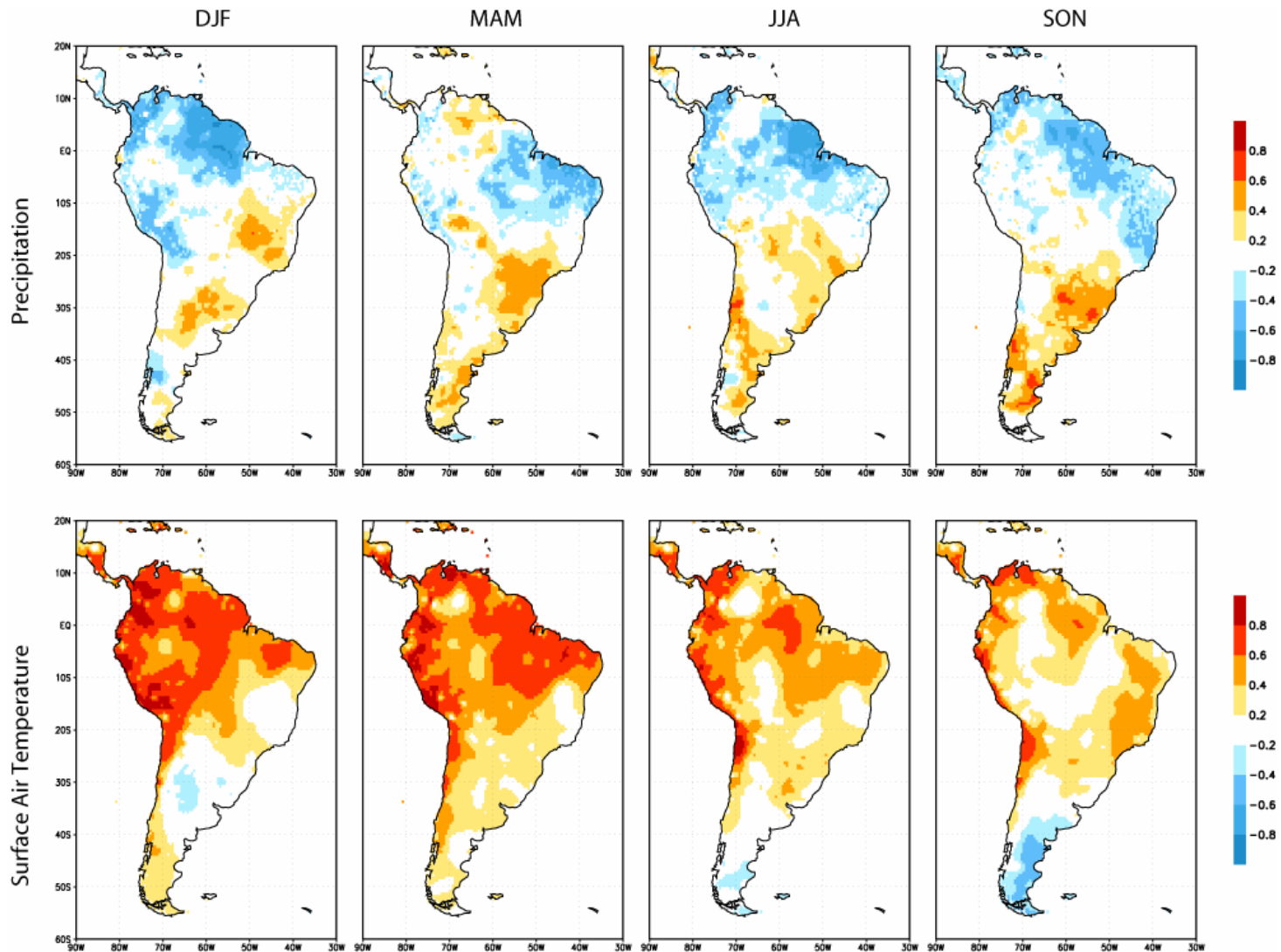
$\Delta\text{lat} \sim \Delta \text{lon} \sim 1^\circ - 3^\circ$

$\Delta z \sim 1 \text{ km}$

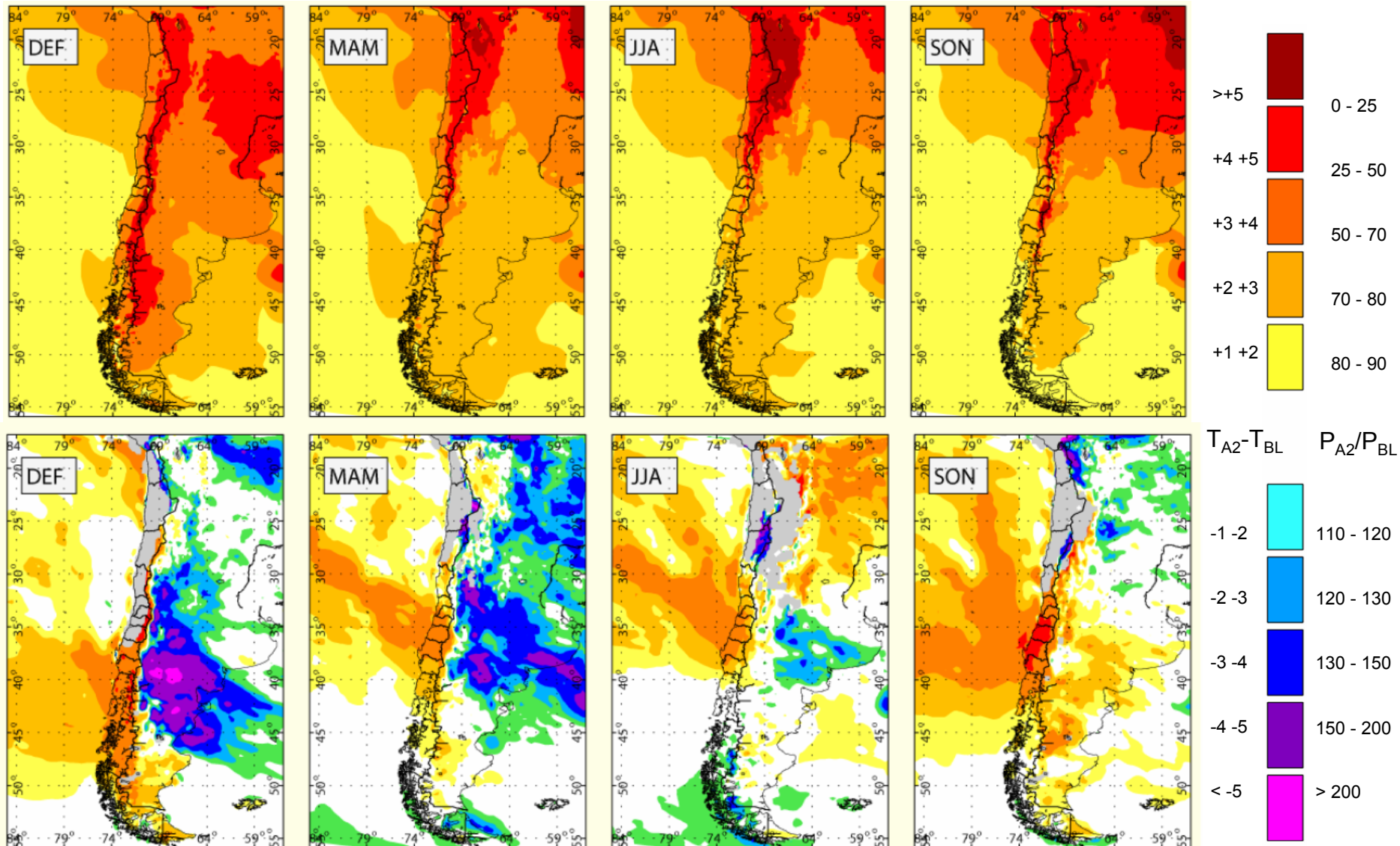
$\Delta t \sim \text{ minutes-hours}$

Top of atmosphere: 15-50 km

Seasonal correlation between Precip/SAT and Multivariate ENSO Index (50 years of data)



Projected Changes PRECIS-DGF



Futuro: 2071-2100 / Presente: 1960-1990